

1

2 Wind-induced collapse of the biopolymeric surface microlayer induces sudden
3 changes in sea surface roughness

4 *Anja Engel*^{1,2*}, *Gernot Friedrichs*^{2,3,4}, *Kerstin E. Krall*⁵, *Bernd Jähne*^{5,6}

5

6 [1] GEOMAR Helmholtz Centre for Ocean Research, Kiel, Germany

7 [2] ~~Christian Albrechts~~ Kiel University ~~of Kiel,~~ (CAU), Germany

8 [3] Institute of Physical Chemistry, Kiel, Germany

9 [4] KMS Kiel Marine Science-Centre for Interdisciplinary Marine Science, Kiel University, Kiel, Germany

10 [5] Institute of Environmental Physics (IUP), Heidelberg University, Heidelberg, Germany

11 [6] Interdisciplinary Center for Scientific Computing (IWR), Heidelberg University, Heidelberg, Germany

12

13 *Correspondence to:* Anja Engel (aengel@geomar.de)

14

15

16

17

18

19 **Abstract:**

20 All exchange between the ocean and atmosphere has to cross the sea surface microlayer (SML), yet the SML
21 impact on modulating air-sea exchange rates remains poorly understood. Surfactants, including biopolymers, can
22 influence exchange rates by altering the rheological properties of the SML, damping surface turbulence, and
23 capillary wave ~~formations~~formation. We investigated the impact of wind speed on SML biopolymer enrichment,
24 surface roughness, and interfacial surfactant coverage at the Heidelberg ‘*Aeolotron*,’ a large annular wind-wave
25 facility filled with 18.000L seawater. Our results show that biopolymer enrichment, specifically the enrichment of
26 polypeptides and polysaccharides, in the SML declined sharply at wind speeds above 6 m/s, coinciding with a
27 sudden increase in the Mean Square Slope (MSS) of waves by 1–2–3 orders of magnitude. At wind speed < 6 m s⁻¹
28 ¹ biopolymer enrichment in the SML was accompanied by high surfactant surface coverage and strongly reduced
29 MSS values ~~by up to two orders of magnitude~~ compared to non-enriched or essentially surfactant-free clean, ~~i.e.~~
30 freshwater, surfaces, indicating a substantial impact of ~~biopolymers~~biopolymer enrichment in the SML for air-sea
31 exchange at lower wind speed. Selective SML enrichment was observed, particularly for the amino acids arginine
32 and glutamic acid, and the amino sugar galactosamine. Amino acid and carbohydrate monomers in the SML also
33 exhibited significant and compound-specific wind-induced variability. Our findings suggest that biopolymers,
34 particularly those derived from bacterial production, accumulate in the SML and act as powerful biosurfactants.
35 Unlike artificial surfactant films, natural SML components were more susceptible to wind-induced disruption and
36 to microbial production and decomposition. Our findings reveal that ecological processes actively regulate the
37 chemical and physical properties of the SML, including surfactant surface coverage, and thereby potentially
38 ~~modulating~~modulate air–sea heat and mass exchange.

39

40

41

42

43

44

45

46

47

48 **1. Introduction**

49 All exchange between the ocean and atmosphere traverses a thin upper ocean boundary layer known as the sea
50 surface microlayer (SML) (Cunliffe et al., 2013; Engel et al., 2017). Less than 1mm thick, the SML is the
51 chemically and structurally complex organic interface layer right below the air-sea interface with distinct physical,
52 chemical, and biological properties, often enriched in high molecular weight biopolymers and surface-active
53 agents (surfactants). These surfactants are amphiphilic molecules with both hydrophilic (water-attracting) and
54 hydrophobic (water-repelling) groups. ~~Under low-wind conditions and due to microscale (capillary) wave~~
55 ~~damping and reduced sun glittering caused by coherent patches of surfactants, organic matter, the~~ accumulation
56 ~~of organic material and surfactants~~ in the SML ~~becomes visible as slicks, i.e. dampens capillary waves and reduces~~
57 ~~light reflection, making the SML appear~~ smooth ~~spots, a phenomenon often referred to as a slick. In the ocean,~~
58 ~~slicks appear shiny, calm, or stripes at darker than~~ the surrounding water ~~surface because they reflect sunlight~~
59 ~~differently.~~

60 Various biochemicals, including heteropolymers of lipids, amino acids, and carbohydrates, contribute to the
61 oceanic surfactant pool (Cunliffe et al., 2013, Gašparović and Čosović, 2003). For example, in
62 lipopolysaccharides, the carbohydrate and lipid moieties represent the hydrophilic and the hydrophobic parts of
63 the molecule. Surfactants can impede air-sea gas exchange by modifying the surface rheological properties of the
64 SML. Specifically, surfactants increase the surface elasticity and effective surface viscosity of water, ~~reducing~~
65 ~~turbulent energy dissipation and damping. As a result, Marangoni stresses arise from surface-tension gradients.~~
66 ~~This damps~~ the formation of capillary waves, which reduces small-scale roughness, and leads to a stronger
67 turbulent energy dissipation near the surface (Wei and Wu, 1992; Frew et al., 1990; Jenkinson et al., 2018; Laxague
68 et al., 2024). ~~Hereby~~ In this context, the overall effect of ~~the~~ surfactants ~~results~~ arises from ~~intricate complex and~~
69 ~~dynamic and~~ competitive adsorption: an excess of highly surface-active compounds inhibits the adsorption of less
70 active surfactants, while a deficiency promotes the contribution of the latter (Pogorzelski et al., 2006; Frka et al.,
71 2012). In the open ocean, organic matter derived from phytoplankton production contains surfactants (Croot et al.,
72 2007; Frew et al., 1990; Wurl et al., 2011). Regions with elevated primary production are therefore expected to
73 have higher surfactant concentrations (Wurl et al., 2011). However, chlorophyll a (Chl *a*), often used as a proxy

74 for primary production, may not accurately predict surfactant occurrence (Laß et al., 2013; Sabbaghzadeh et al.
75 2017). Instead, a mixture of more recalcitrant dissolved organic matter (DOM) and freshly produced biopolymers
76 seems to control surfactant dynamics in the SML (Barthelmeß and Engel, 2022). Certain strains of heterotrophic
77 bacteria produce surfactants (Satpute et al., 2010) and have also been associated with surfactant-covered ocean
78 surfaces (Kurata et al., 2016). ~~Besides~~In addition, surfactants present in seawater have ~~also been linked to~~
79 ~~anthropogenic~~associated with human-related and terrestrial sources, ~~including rivers such as riverine~~ runoff (Cuscov
80 and Muller, 2015; Shararom et al., 2018).

81 ~~Due to the variability~~Variability of surfactants in the SML, ~~is likely one of the main reasons why~~ parameterizations
82 based solely on wind speed struggle to accurately predict mass and momentum exchange between the sea and
83 atmosphere, particularly at low wind speeds where the number of observations is small (Wanninkhof et al., 2009;
84 Nagel et al., 2019). This significantly hinders accurate estimates of the ocean's contribution to the cycling of
85 greenhouse gases. For example, a substantial reduction of air-sea fluxes of CO₂ has been documented under high
86 accumulation of natural surfactants ~~in~~using surface seawater of the Atlantic in an on-board air-sea gas exchange
87 tank experiment (Pereira et al., 2018). In association with cyanobacteria blooms (*Trichodesmium* sp.) in the Baltic
88 Sea, a drastic reduction of the gas transfer coefficient (k_w) was associated with bloom-induced biosurfactants,
89 leading to $\pm 20\%$ differences in seasonal CO₂ uptake estimates (Schmidt and Schneider, 2011). Another study in
90 the eastern tropical North Atlantic indicated that surfactants, especially in areas of high biological productivity,
91 may dampen the air-sea exchange of other greenhouse gases like N₂O as well (Kock et al., 2012). Estimates on
92 how surfactants in the SML reduce global net oceanic CO₂ uptake vary between 15% and 60% (Pereira et al.,
93 2018; Asher et al., 1997; Tsai and Liu, 2003; Wurl et al., 2016). However, at sea, the variability and complexity
94 of organic matter composition, combined with a dynamic physical environment, including waves, rain, and varying
95 wind speed, make it hard to directly quantify the influence of surfactants on air-sea gas exchange and to examine
96 which biochemical components contribute to the surfactant pool. Repeated conditions of constant wind speeds,
97 especially in the low wind regime, are challenging to meet in the open ocean.

98 To investigate the influence of wind speed and surfactants on air-water mass exchange under more controlled
99 conditions, wind-channel experiments have typically been conducted using freshwater and defined additions of
100 artificial surfactants such as oleyl alcohol, hexadecanol, Triton-X and hexadecylamine (Hühnerfuss et al., 1981;
101 Jähne, 1987, Alpers and Hühnerfuss, 1989; Mesarchaki et al., 2015; Frew et al., 1995; Gade et al., 1998; Krall,
102 2013). These studies demonstrated strong wave damping of surfactants up to a wind speed of 13 m s⁻¹ (Broecker
103 et al., 1978; Jähne, 1987). Only a limited number of wind-channel experiments have been conducted using natural

104 surface films and seawater ~~(. For example, Tang and Wu, (1992; Ribas-Ribas et al., 2018). These studies)~~
105 demonstrated the wave-damping capacity of natural films under varying wind speeds, but did not investigate the
106 biochemical composition of the surfactants.

107 ~~This study aimed~~ Contributing to a joint effort to close this knowledge gap, by conducting an experimental
108 campaign at the Heidelberg *Aeolotron*, a unique large-scale facility capable of generating controlled wind
109 conditions of up to 22 m/s, which we filled with ~~approx. 18.000L~~ 18000L natural seawater. Unlike previous
110 investigations that relied largely on artificial surfactants, freshwater, or simplified laboratory systems, our
111 approach allowed us to directly examine natural marine biochemicals under controlled yet realistic SML
112 conditions. Specifically, we investigated how wind speed influences the enrichment of the two quantitatively most
113 abundant biopolymer classes, total hydrolysable amino acids (THAA) and total combined carbohydrates
114 (TCCHO), in the SML and how these biopolymers contribute to capillary wave damping. To further link SML
115 composition to surface physical properties, we also quantified ~~surfactant concentrations~~ surface roughness in terms
116 of mean square slope measurements and surfactant surface coverage.

118 1. Material and Methods

119 2.1 Experimental conditions and treatments

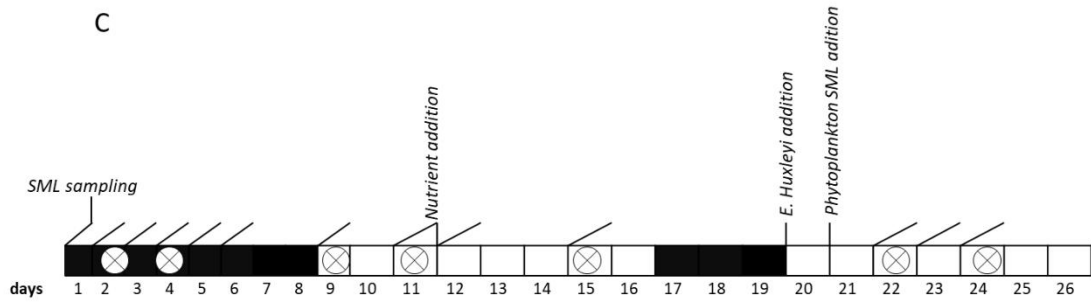
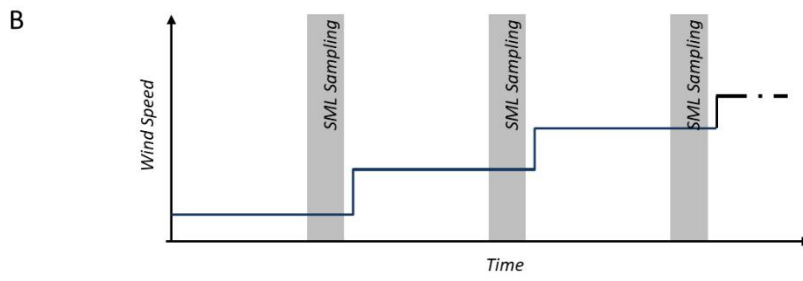
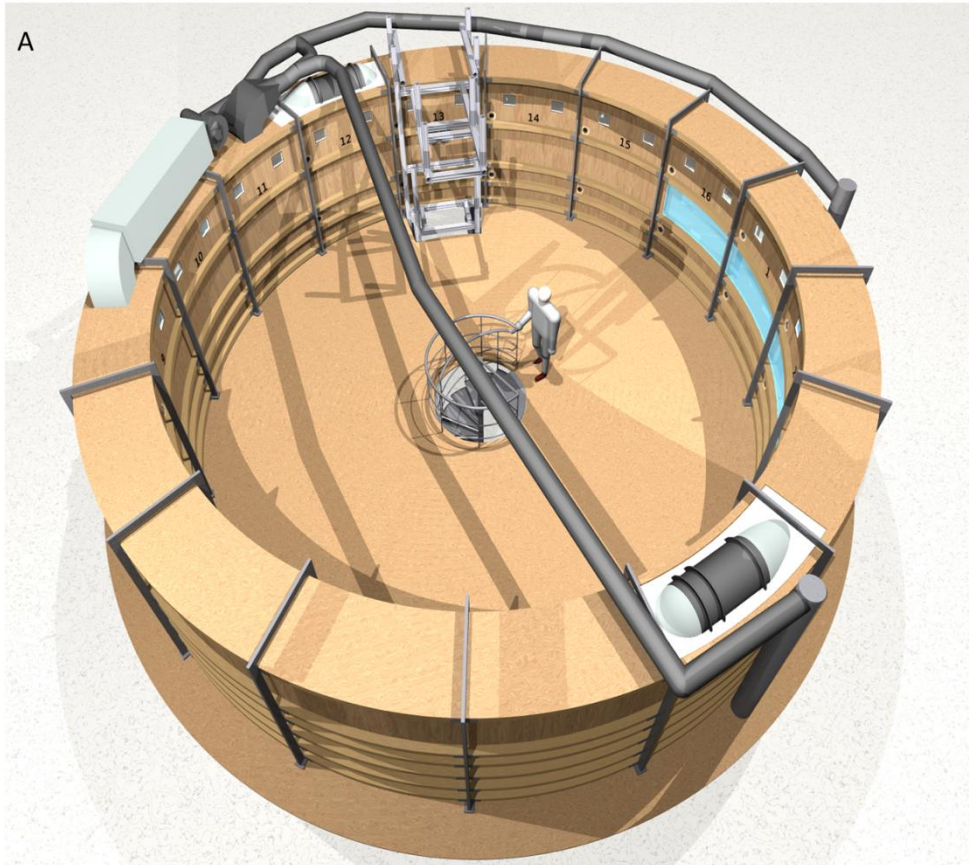
120 This study was part of the larger ‘*Aeolotron*’ experiment, conducted in November 2014 to investigate various air-
121 sea exchange processes under controlled wind conditions. The *Aeolotron* is an annular wind wave tank in
122 Heidelberg, Germany, with a diameter of approximately 10 m, a water depth of 1 m ~~with~~ a 1.4m air space above
123 the water, and a total surface area of 18.4 m² (Figure 1A).

124 Due to its unique annular geometry, the *Aeolotron* wind-wave tank offers distinct advantages over conventional
125 linear wind-wave tanks when aiming to replicate ocean-like conditions ~~(Schmundt et. al, 1995)~~. In linear tanks,
126 surfactants tend to accumulate near the wave absorber and are eventually rendered inactive, as they are transported
127 out of the active measurement region by wind and wave action. In contrast, the annular design of the *Aeolotron*
128 ensures that surface films remain uniformly distributed, allowing for sustained and realistic interactions at the air-
129 water interface. Additionally, while conventional linear tanks are limited by fetch, the *Aeolotron* permits the
130 continuous development of wind waves along an effectively unlimited fetch, allowing for the generation of older,

131 more ocean-like wave fields. This enables the study of processes that are otherwise difficult to capture in shorter
132 linear facilities.

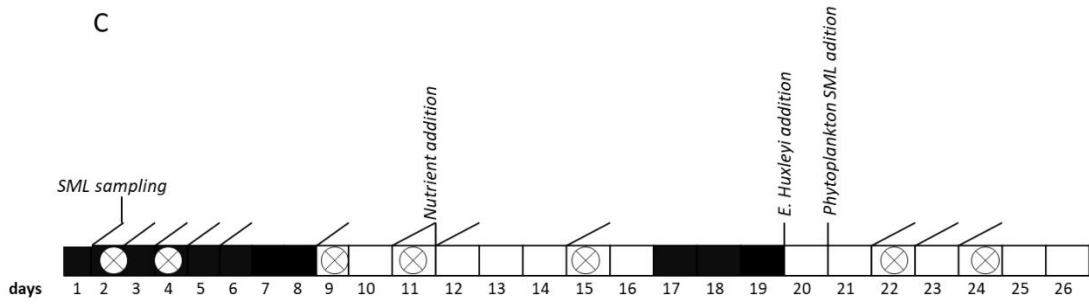
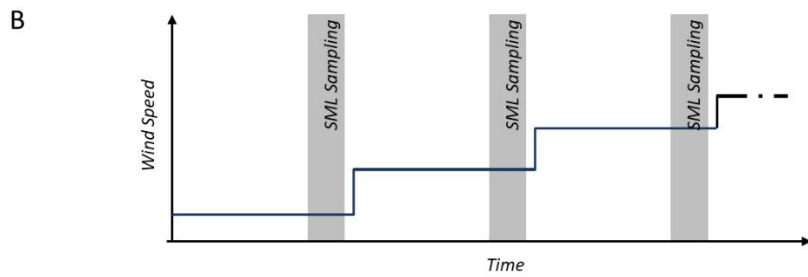
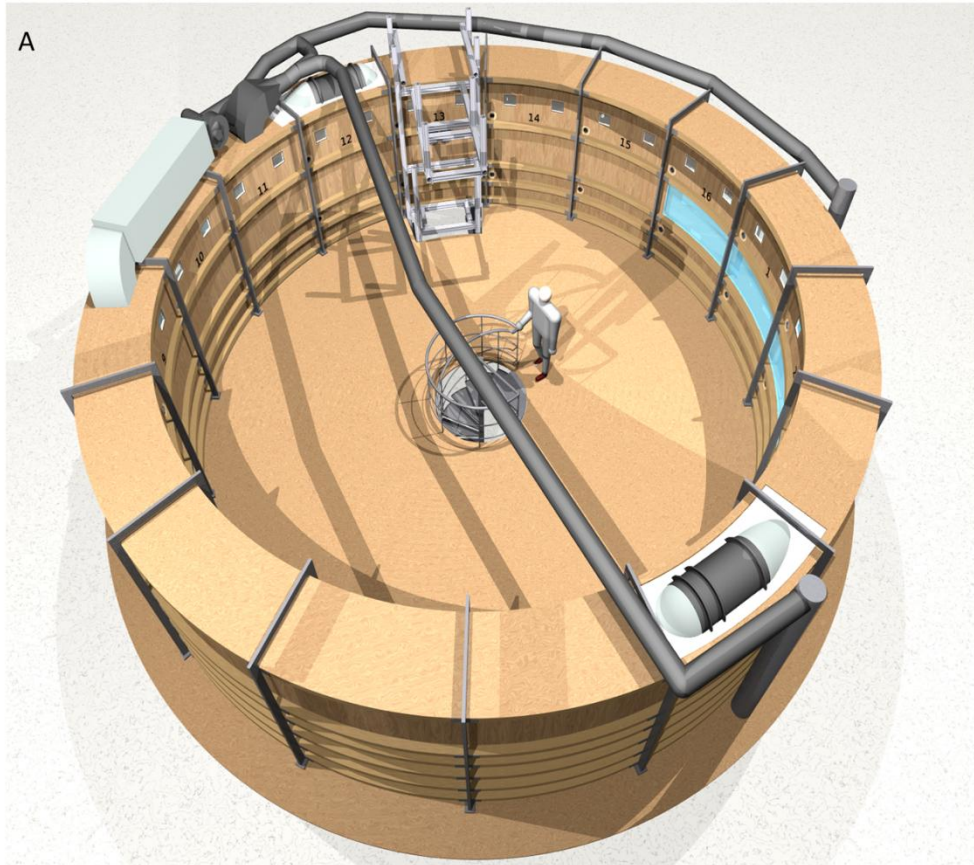
133 Importantly, the limited absolute size of the *Aeolotron* does not compromise its relevance for studying interfacial
134 gas exchange processes. The key mechanisms governing air-sea gas exchange, particularly those involving the sea
135 surface microlayer (SML), operate on length scales of millimetres or less. These include molecular diffusion,
136 micro-scale turbulence, and surfactant-mediated suppression of short capillary waves, all of which are fully
137 resolved within the *Aeolotron*'s experimental framework- [\(Schmundt et al., 1995; Mesarchaki et al., 2015\)](#). As
138 such, the *Aeolotron* provides an excellent platform for investigating the fundamental physics of gas transfer and
139 interfacial dynamics under highly controlled yet ocean-relevant conditions.

140 The setup of the *Aeolotron* experiment and the physical, chemical and biological treatments in the course of the
141 experiment are described in more detail elsewhere (Engel et al., 2018). Briefly, the wind wave channel was filled
142 with approximately 18000 L of seawater, which had been collected in September 2014 in the North Atlantic and
143 German Bight, North Sea. The seawater had been stored in the dark at 10°C [for about a month](#) until it was used to
144 fill the *Aeolotron*.



145

146



147

148 **Figure 1, A-C: Top-view on the Heidelberg annular wind-wave channel *Aeolotron* (A), where experiments**
149 **with increasing wind speed were conducted on seven days. Step-wise increase in wind speed applied**
150 **during each wind experiment (B) and timeline of the *Aeolotron* study with different seawater**
151 **modifications and the seven wind experiments (crossed circles) (C).**

152 Seawater temperature within the *Aeolotron* ranged from 20.13 to 22.21°C. Light sources were operated over the
153 tank for two periods of eight (days 7-16) and six days (days 20-26), providing a photon flux of 115-120 $\mu\text{mol m}^{-2}$
154 s^{-1} . Inorganic nutrients were added on day 12. About 800 ml of a culture of *Emiliana huxleyi* (cell density: $4.6 \times$
155 10^5 cell ml^{-1}) was added on day 20. In addition, 6L of biogenic microlayer ~~from sampled with the glass plate during~~
156 a previous phytoplankton mesocosm experiment, stored frozen at -20°C for about 6 months, was thawed and added
157 on day 21. The total duration of the *Aeolotron* experiment was 26 days.

158

159 During the ~~Aeolotron~~*Aeolotron* experiment, a total of 7 wind experiments were conducted on days 2, 4, 9, 11, 15,
160 22, and 24 (Figure 1B, C). During each experiment, the wind speed was increased stepwise yielding a range of
161 wind ~~speeds~~ speeds (U_{10}) from ~~about 1.3~~ m/s to ~~18.721.9~~ m/s. The duration of each wind speed setting varied from
162 30 min to 2 hrs, with longer durations for the lower wind speeds. This scheme was chosen to facilitate robust
163 concurrent measurements of air-sea gas exchange for each wind speed condition in a parallel project (Mesarchaki
164 et al., 2015).

165 Wind speeds during the experiments were measured using a Pitot tube, and water velocities were measured using
166 an acoustic Doppler velocimeter mounted equidistant from both the outer and inner wall at a water depth of
167 approximately 50 cm. The friction velocity U_* , a measure for the wind's momentum input into the water, was
168 calculated from the water velocity using a momentum balance method (Bopp, 2014). The friction velocity U_*
169 measured in the *Aeolotron* was subsequently converted to U_{10} using a parametrization of the drag coefficient
170 derived from the open ocean (Edson et al., 2013). ~~At the lowest wind speeds studied, the measured velocities in~~
171 ~~the water were close to or at the resolution limit of the velocimeter. For these conditions, no friction velocity and,~~
172 ~~thus, no wind speed U_{10} could be obtained.~~

173

174 2.2 Wave Slope Measurement

175 The Mean Square Slope (MSS, a statistical dimensionless parameter for surface roughness) of the water surface is
176 strongly correlated with the air-sea gas transfer velocity (Jähne et al., 1987; Frew et al., 2004). The MSS is,
177 therefore, an important parameter linking sea surface properties to air-sea exchange processes. During this study,
178 the MSS of wind-induced waves was computed from wave slope images (Kiefhaber et al., 2014). These images
179 were taken by a high-speed camera, positioned in a telecentric setup above the water surface, capturing images of
180 a wave-height independent area at the water surface measuring 16 cm x 20 cm, achieving a resolution of 0.22
181 mm^2/pixel at a rate of 1500 frame per second. Illumination of the water body was achieved from below, utilizing
182 a programmable high-power LED light source in such a way that both the along-wind and cross-wind slopes, s_x

183 and s_y of the waves, could be computed. From the slope images, the MSS is simply computed as an average over
184 space and time, $MSS=(s_x^2 + s_y^2)$. As a reference, the variation of MSS with wind speed was determined for clean
185 freshwater in a separate Aeolotron studiesstudy beforehand (Krahl, 2013; Kunz, 2017). Uncertainties for MSS
186 values are <10% for values >0.002. Close to the detection limit of 0.0003, uncertainties are in the order of the
187 measured value.

188

189 2.3 Sampling

190 The SML was sampled ~~at~~on 12 days in the morning at low wind speed (U_{10} : 1.3-1.5 $m\ s^{-1}$) and towards the end
191 of each wind speed step during each of the seven wind experiments (Figure 1B). Sampling was carried out using
192 the glass plate technique in accordance with established protocols (Cunliffe and Wurl, 2014), employing a
193 borosilicate glass plate ($500 \times 250 \times 5$ mm) and a Teflon wiper. For sampling, the glass plate was inserted
194 perpendicular to the surface and withdrawn at a rate of ~ 20 cm/sec. Subsequently, the sample, retained by surface
195 tension, was removed utilizing a Teflon wiper. Each sampling involved between 23 and 48 dips and precise
196 documentation of the number of dips and total volume collected. All samples were collected in acid-cleaned (10%
197 HCl) glass bottles, washed with ultrapure water from a Milli-Q ~~system~~system, and rinsed with 20 mL of sample
198 initially. Before each sampling event, both the glass plate and wiper were cleaned with 10% HCl and extensively
199 rinsed with Milli-Q water.

200 The thickness (d , μm) of the SML sampled with the glass plate was approximated:

$$201 \quad (1) \quad d=V/(A \times n)$$

202 where V represents the collected SML volume (ranging from 200-420 mL), A denotes the sampling area of the
203 glass plate ($A = 2000$ cm^2), and n is the number of dips (Cunliffe and Wurl, 2014). In this study, d serves as an
204 operational estimate for the thickness of the SML and is referred to as apparent SML thickness-.

205 Underlying water (ULW) samples were taken in the morning at low wind speed from a tap ~ 50 cm below the water
206 surface, representing half the water column's height. These samples, ~ 500 ml each, were filled into 10% HCl-
207 cleaned borosilicate glass bottles, rinsed with Milli-Q water, and pre-rinsed with ~ 20 mL of the sample directly
208 before filling. ULW samples were collected daily between day 1 and day 26 of the experiment, except for day 6
209 (Figure 1C).

210

211 2.4 Analysis of organic compounds

212 2.4.1 Dissolved organic carbon (DOC)

213 -Samples for DOC (20 ml) were collected in duplicate from the SML and ULW and filled into combusted glass
214 ampoules after filtration through combusted glass-fibre filters (GF/F) filters (8 hours, 500° C). Samples were
215 acidified with 80 µL of 85% phosphoric acid, heat sealed immediately, and stored at 4°C in the dark until analysis.
216 DOC samples were analyzed by applying the high-temperature catalytic oxidation method (TOC -VCSH,
217 Shimadzu) (Engel and Galgani, 2016). The instrument was calibrated every 8-10 days by measuring standard
218 solutions of 0, 500, 1000, 1500, 2500 and 5000 µg C L⁻¹, prepared from a potassium hydrogen phthalate standard
219 (Merck 109017). Every measurement day, Milli-Q water was used to determine the instrument blank, which was
220 accepted for values <12 µg C L⁻¹. DOC analysis was validated on every measurement day with deep seawater
221 reference (DSR) material provided by the Consensus Reference Materials Project of RSMAS (University of
222 Miami) yielding values within the certified range of 42-45 µmol C L⁻¹. Additionally, two internal standards with
223 DOC within the range of those in samples were prepared each measurement day using a potassium hydrogen
224 phthalate (Merck 109017). DOC concentration was determined in each sample from 5 to 8 injections. The precision
225 was <4%, estimated as the relative standard deviation of replicate measurements.

226 2.4.2 Biopolymers

227 Total hydrolysable amino acids (THAA), i.e., amino acids with a peptide bond, including amino acids contained
228 in polypeptides or heteropolymers, like lipopeptides and glycopeptides, were determined in ULW and SML
229 (Lindroth and Mopper, 1979; Dittmar et al, 2009). 5 mL of sample were filled into pre-combusted glass vials (8
230 hours, 500°C) and stored at -20 °C until analysis. Duplicate samples were hydrolyzed for 20h at 100°C with HCl
231 (30% suprapur, Merck) and neutralized by acid evaporation under vacuum in a microwave at 60°C. Samples were
232 washed with Milli-Q water to remove the remaining acid. Analysis was performed on a 1260 HPLC system
233 (Agilent). Thirteen different amino acids were separated with a C18 column (Phenomenex Kinetex, 2.6 µm, 150
234 x 4.6 mm) after in-line derivatization with o-phthalaldehyde and mercaptoethanol. The following standard amino
235 acids were used: aspartic acid (ASX), glutamic acid (GIX), serine (SER), arginine (ARG), glycine (GLY),
236 threonine (THR), alanine (ALA), tyrosine (TYR), valine (VAL), phenylalanine (PHE), isoleucine (ILEU), leucine
237 (LEU), γ- aminobutyric acid (GABA). α- aminobutyric acid was used as an internal standard to account for losses
238 during handling. Solvent A was 5% Acetonitrile (LiChrosolv, Merck, HPLC gradient grade) in
239 Sodiumdihydrogenphosphate (Merck, suprapur) Buffer (PH 7.0), Solvent B was Acetonitrile. A gradient was run

240 from 100% solvent A to 78% solvent A in 50 minutes. The detection limit for individual amino acids was 2 nmol
241 monomer L⁻¹. The precision was <5%, estimated as the relative standard deviation of replicate measurements.
242 Based on THAA measurement, the Degradation Index (DI) was calculated as an indicator of the diagenetic status
243 of organic matter (Dauwe and Middelburg, 1998). For instance, leucine typically exhibits preferential
244 degradation compared to glycine. Mole percentages of amino acid were standardized using averages, and
245 standard deviations and multiplied with factor coefficients based on Principal Component Analysis (PCA) as
246 given in Dauwe et al. (1999). Lower ~~values~~-DI values indicate more degraded; organic matter, whereas higher DI
247 values indicate more fresh organic matter.

248
249 Total hydrolysable carbohydrates > 1 kDa (TCHO), i.e., carbohydrates with a glycosidic bond, including
250 carbohydrates contained in polysaccharides and heteropolymers like glycolipid and glycopeptides, were
251 determined in bulk seawater and in the SML. 20 mL were filled into pre-combusted glass vials (8 hours, 500 °C)
252 and kept frozen at -20 °C until analysis. The analysis was conducted by applying high-performance anion exchange
253 chromatography coupled with pulsed amperometric detection (HPAEC-PAD) on a Dionex ICS 3000 (Engel and
254 Händel, 2011). Samples were desalinated by membrane dialysis (1 kDa MWCO, Spectra Por) for 5 h at 1 °C,
255 hydrolyzed for 20 h at 100°C with 0.4 M HCl final concentration, and neutralized through acid evaporation under
256 vacuum and nitrogen atmosphere (1h, 60 °C). Two replicate samples were analyzed. For our system, the best
257 resolution of sugars was obtained at 25 °C and, therefore, applied constantly during all analyses. In order to
258 minimize degradation of samples before analysis, the temperature in the autosampler was kept at 4 °C. The system
259 was calibrated with a mixed sugar standard solution including the neutral sugars: fucose (4.6 µM, FUC), rhamnose
260 (3.1 µM, RHA), arabinose (2.0 µM, ARA), galactose (2.4 µM, GAL), xylose/ mannose (3.1 µM, XYL/ MAN),
261 glucose (2.4 µM, GLC), amino sugars: galactosamine (2.0 µM, GAL-N), glucosamine (2.8 µM, GLC-N), and
262 acidic sugars: galacturonic acid (2.8 µM, GAL-URA), gluconic acid (5.1 µM, GLC-AC), glucuronic acid (3.0 µM,
263 GLC-URA) and muramic acid (1.9 µM, MUR-AC). Regular calibration was performed by injecting 12.5 µl, 15.0
264 µl, 17.5 µl and 20 µl of mixed standard solution. The linearity of the calibration curves of individual sugar
265 standards was verified in the concentration range 10 nM-10 µM. Therefore, the standard mixture was diluted 10,
266 20, and 50-fold with Milli-Q water. The injection volume for samples and for the blank was 17.5 µl. To check the
267 performance of carbohydrate analysis and stability of the HPLC-PAD system, a 17.5 µl standard solution was
268 analyzed after every second sample. The detection limit was 10 nmol L⁻¹ for each sugar, with a standard deviation
269 between replicate runs of <2%. Milli-Q water was used as a blank to account for potential contamination during

270 sample handling. Blanks were treated and analyzed in the same way as the samples. Blank concentration was
 271 subtracted ~~from~~from the sample concentration if above the detection limit.

272 The relative concentration of a substance (A) in the SML was compared to its concentration in ULW by the
 273 enrichment factor (EF):

$$274 \quad (4) \quad EF = (A)_{SML} / (A)_{ULW}$$

275 Because of normalization, EFs for different components can be readily compared. Enrichment of a component is
 276 indicated by $EF > 1$, depletion by $EF < 1$. Statistical analyses were conducted using SigmaStat 4.0.

277

278 2.4.3 Surfactant Coverage and Enrichment

279 Samples for surfactant coverage (sc) were taken only for the initially low and at the highest wind speed. Duplicate
 280 50 mL SML samples were collected on 7 experimental days (days 2, 4, 9, 11, 15, 22, and 24). ~~On~~ for initially low
 281 and at the highest wind speed; on day 2, only a low wind sample was available. The SML samples were transferred
 282 into polypropylene bottles, immediately frozen at -40°C for transport, and stored at -80°C before analysis using
 283 surface-sensitive non-linear vibrational sum-frequency generation (VSFG) spectroscopy with a commercial
 284 picosecond VSFG spectrometer (EKSPLA, 532 nm up-conversion wavelength). ~~The use of VSFG spectroscopy~~
 285 for SML surfactant analysis and its interpretation has been shown previously (Engel et al., 2018; Laß and
 286 Friedrichs, 2011). The VSFG signal intensity $I_{VSFG, SML}$ (integrated over the spectral wavenumber range of C-H
 287 bond signatures, $2750\text{ cm}^{-1} - 3000\text{ cm}^{-1}$) can be related to the surfactant surface coverage (~~sc~~) via a square root
 288 relationship (~~$\sqrt{I_{VSFG, SML}} / \sqrt{I_{VSFG, DPPC}} \propto$~~ $\sqrt{I_{VSFG, SML}} / \sqrt{I_{VSFG, DPPC}} \propto sc$), where $I_{VSFG, DPPC}$ refers to the intensity of
 289 a well-defined reference surfactant monolayer, here an artificial monolayer of the phospholipid
 290 dipalmitoylphosphatidylcholine (DPPC), a well-characterized and chemically stable model surfactant. In our
 291 previous work, which focused on the correlation of low wind speed data with the concentration of γ -aminobutric
 292 acid (GABA) as an indicator for microbial decomposition (Engel et al., 2018), we have used a highly compressed
 293 monolayer of DPPC in its solid 2D phase as the $\sqrt{I_{VSFG, DPPC}}$ reference signal for a completely surfactant-covered
 294 surface. However, as the complex mixture of biosurfactants will prevent the formation of such a highly ordered
 295 monolayer, we now have adopted the onset of the DPPC 2D phase transition

296 In order to convert sc into an effective concentration ~~of measure for~~ surfactants in the SML and thus enable a direct
 297 correlation with the measured concentration trends of the DOM fractions THAA and TCHO, the exact composition
 298 and surfactant properties of the substances present in the SML would have to be known. However, for a surfactant
 299 pool typically dominated by wet (i.e., “soluble” in contrast to “unsoluble” dry) surfactants (Laß and Friedrichs,
 300 2011), it is reasonable to assume an adsorption equilibrium of bulk SML surfactants with the air-water interface
 301 such that sc can be described by a reduced Langmuir isotherm (Burrows et al., 2014) according to:

$$302 \quad (2) \quad sc = \frac{c^*}{1-c^*} \quad \text{or} \quad (3) \quad c^* = \frac{sc}{1+sc}$$

303 Here, c^* is the reduced concentration $c^* = c/c_{1/2}$ with $c_{1/2}$ corresponding to the effective bulk SML surfactant
 304 concentration yielding a half-covered surfactant monolayer. Accordingly, sc increases linearly with c^* at low
 305 surfactant concentrations but levels out towards the limiting value of a completely covered surface at high
 306 surfactant concentrations. While the surfactant indices c^* and sc derived from the VSFG measurements, provide
 307 semi-quantitative insights into surfactant abundance and surface coverage, it is important to note that they are
 308 based on assumptions and approximations and should be interpreted accordingly. For example, the analysis may
 309 be biased by the variable composition of the surfactant pool during the *Aeolotron* study. This may have induced
 310 more or less pronounced variations in the effective $c_{1/2}$ value, which, however, was assumed to be constant.

311

312 **2.5 Data analysis**

313 ~~The relative concentration of a substance (A) in the SML was compared to its concentration in ULW by the~~
 314 ~~enrichment factor (EF):~~

$$315 \quad (4) \quad \text{EF} = (A)_{\text{SML}} / (A)_{\text{ULW}}$$

316 ~~Because of normalization, EFs for different components can be readily compared. Enrichment of a component is~~
 317 ~~indicated by $\text{EF} > 1$, depletion by $\text{EF} < 1$. Statistical analyses were conducted using SigmaStat 4.0.~~

318

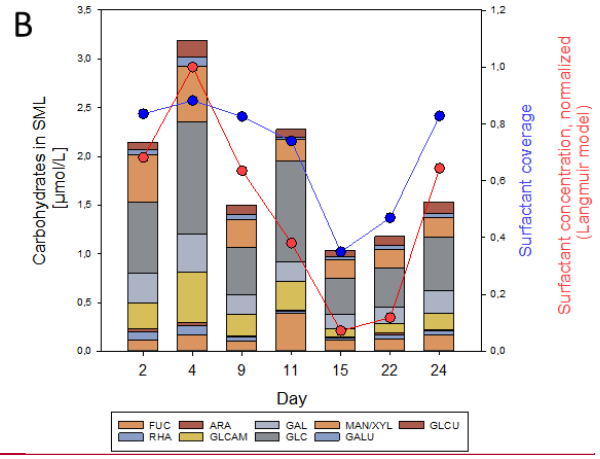
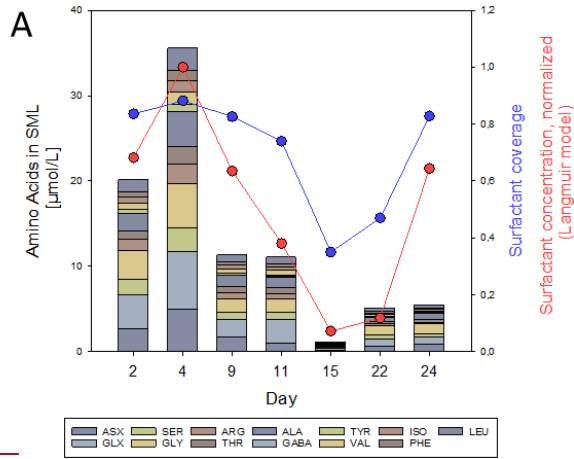
319 **1. Results**

320 **3.1 Organic matter variations in the SML in the course of the *Aeolotron* experiment**

321 Biomass in the water column and variations in microbial abundance and organic matter composition in the course
322 of the *Aeolotron* experiment have been reported previously (Engel et al., 2018). -To illustrate the conditions in
323 which the wind experiments were conducted, we briefly describe the relevant findings here. Particulate organic
324 matter remained low throughout the experiment, with particulate organic carbon (POC) concentrations ranging
325 between 4 and 29 $\mu\text{mol L}^{-1}$. Chlorophyll *a* (Chl *a*) concentration increased after introducing an *Emiliana huxleyi*
326 culture on day 19, reaching peak values of 0.042 $\mu\text{g L}^{-1}$ on day 25. DOC concentration in the bulk seawater
327 increased during the course of the experiment (days 2-24) from 85 $\mu\text{mol L}^{-1}$ to 120 $\mu\text{mol L}^{-1}$. Biopolymers
328 accumulating in the SML can be dissolved, colloidal and particulate. In particular, gel-like particles containing
329 amino acids (~~C~~-Coomassie stainable particles, ~~C~~(CSP) and carbohydrate containing transparent exopolymer particles,
330 ~~(TEP)~~ have been shown to accumulate in the SML. (Sun et al., 2018). To account for these components ~~in~~
331 our analysis, and given that the cellular biomass was generally low, we here report total ~~biochemical~~
332 concentrations ~~of the biochemicals, where~~ THAA ~~ranged~~ from 0.83 to 1.67 $\mu\text{mol L}^{-1}$ and TCHO from 0.66 to
333 1.28 $\mu\text{mol L}^{-1}$.

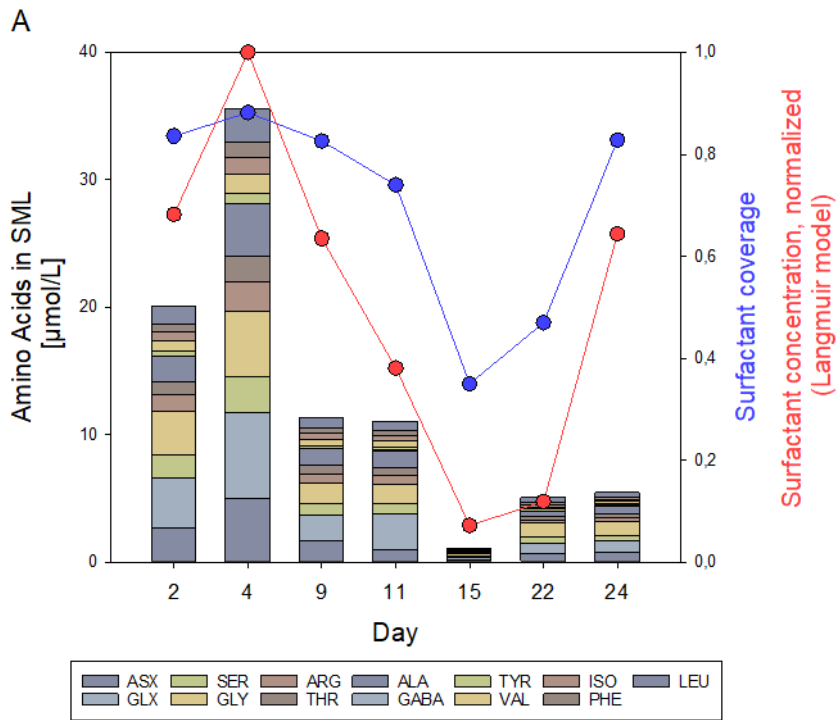
334 Throughout the *Aeolotron* experiment, the SML consistently showed enrichment in DOC, THAA, and TCHO,
335 except on day 15, where the difference between SML and ULW fell within analytical error limits. DOC enrichment
336 factors (EF_{DOC}) ranged from 1.0 to 1.6. THAA concentration in the SML was highest on day 4 with 35.5 $\mu\text{mol L}^{-1}$,
337 declined to ~~the~~ lowest concentration on day 15 (1.05 $\mu\text{mol L}^{-1}$), and increased again after the addition of natural
338 phytoplankton-derived organic matter on days 20 and 21 (Figure 2A). In general, the monomeric composition of
339 THAA in the SML was dominated by GLX (15.8- 25.3 Mol%), GLY (14.2- 21.5 Mol%), and ASX (8.84 – 16.0
340 Mol%). GABA, an indicator for bacterial degradation, was highest on day 15 with 0.41 Mol%. High enrichment
341 of THAA in the SML was observed during the first 11 days of the *Aeolotron* experiment ($\text{EF}_{\text{THAA}}=13-38$). THAA
342 were slightly depleted in the SML on day 15 ($\text{EF}_{\text{THAA}}=0.91$) and became enriched again thereafter ($\text{EF}_{\text{THAA}}=2.89-$
343 3.24). A selective enrichment of individual amino acids in the THAA pool of the SML was observed, with the
344 highest enrichment observed on day 4 for the basic amino acid ARG ($\text{EF}_{\text{ARG}}=74.4$), which contributed only 2.8-
345 6.2 % Mol to the THAA pool, and for the acidic amino acid GLX ($\text{EF}_{\text{GLX}}=53.7$).

346 Organic matter accumulating in the SML was generally less degraded than in the ULW, as indicated by the
347 degradation index (DI) based on THAA composition (Figure S1). This, in turn, suggested that it was the ‘fresher’
348 fraction of biopolymers that became selectively enriched in the SML. In particular, DI values for organic matter
349 in the SML were lowest on day 15, when biopolymer concentration was ~~also~~ lowest ~~also~~, indicating preferential
350 decomposition of the more labile organic matter.

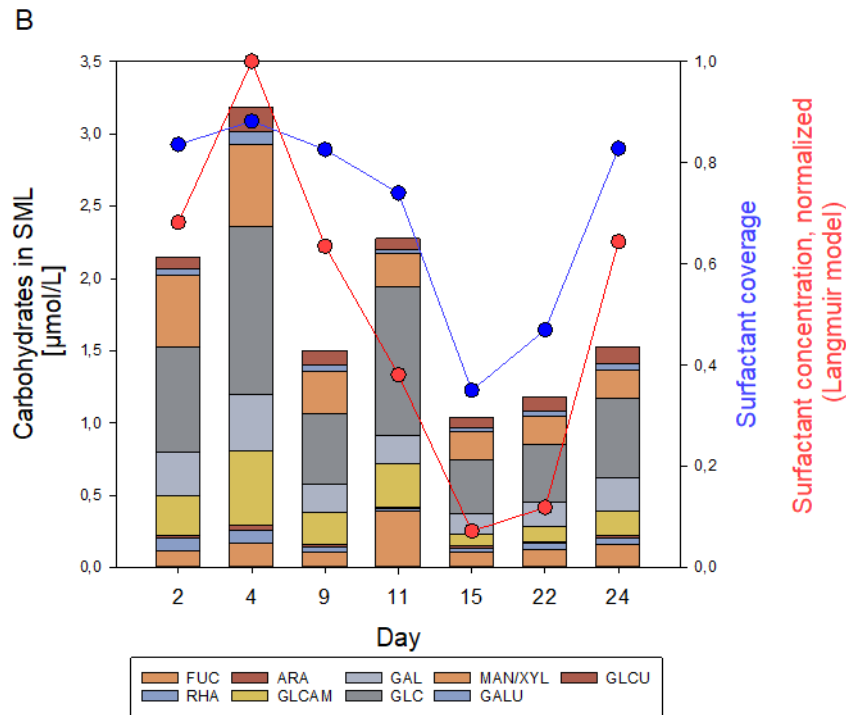


351

352



353



354

355 **Figure 2A, B: Concentration/composition of (a) THAA and (b) THCO in the SML at low initial wind speed**
 356 **(1.3-2.0 ms^{-1}) and variation of surfactant surface coverage (sc , blue circles), as well as normalized reduced**
 357 **bulk SML surfactant concentration (c^*/c_{max} , red circles). Based on a dataset first published in Engel et al.**
 358 **(2018).**

359 TCHO in the SML varied between 2.14 and 1.03 $\mu\text{mol L}^{-1}$, and -similar to THAA- were higher during the first 11
 360 days of the experiment, lowest on day 15, and increased again until day 24, but without reaching the high values
 361 from the first days of the experiment (Figure 2B). TCHO were enriched in the SML with EF_{TCHO} of 1.5–5.6, with
 362 higher values observed during the first four days of the experiment. TCHO composition in the SML was dominated
 363 by GLC (33-45 Mol%), XYL/MAN (10-23%), and GAL (8.8-15 Mol%). FUC has been considered an indicator
 364 of labile, phytoplankton-derived TCHO (Engel et al., 2012). FUC was 5 Mol% at the beginning of the experiment
 365 and increased after the addition of the phytoplankton-derived material to 17 Mol%. Likewise, GLC-N, as an
 366 indicator of more degraded TCHO, decreased from 12.6 Mol% initially to 8 Mol%. Within the pool of TCHO
 367 in the SML, the highest enrichment was observed on day 4 for the amino-sugar GLC-N ($EF_{\text{GLC-N}}=12.89$) and the
 368 acidic sugars GAL-URA and GLC-URA ($EF_{\text{GAL-URA}}= 6.70$, $EF_{\text{GLC-URA}}= 6.57$). On day 22, biopolymer
 369 concentration in the SML had increased again as natural slick material was added on day 21, yielding EF_{TCHO}
 370 values around 3 on days 22 and 24.

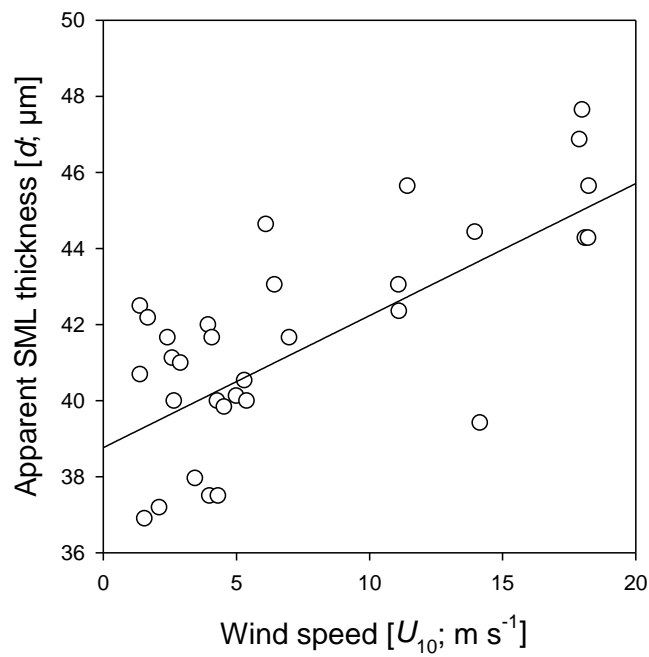
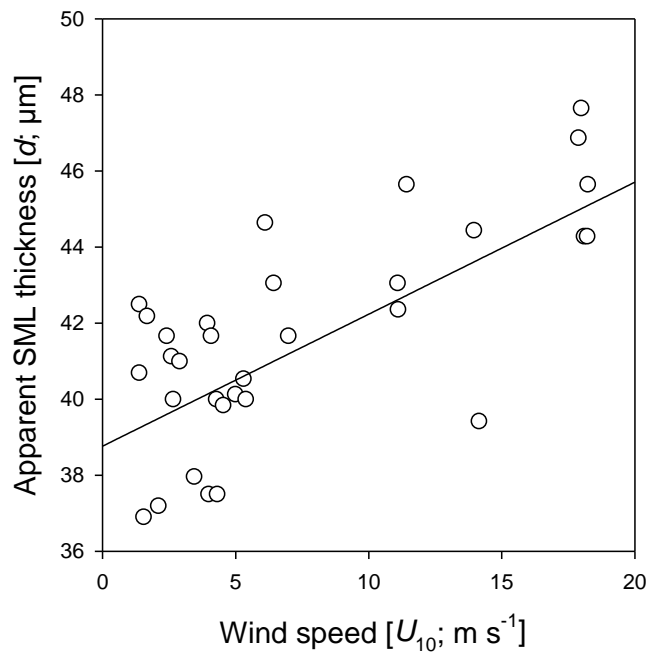
371 The biopolymer ratio [THAA]:[TCHO] was highest on days 2 and 4 with values of 9.4 and 11, respectively, and
372 decreased thereafter. [THAA]:[TCHO] was lowest ~~of~~on day 15 with equal concentrations and yielded 4.3 and 3.6
373 on days 22 and 24.

374 Variations in biopolymers in the SML aligned well with the surfactant surface coverage index sc . Surface coverage
375 was generally high, with $sc > 0.74$ for 5 out of 7 days. The overall similar trend ~~of~~in biopolymer and surfactant
376 abundance was even more evident in the reduced surfactant-concentration data, which have been normalized to
377 the maximum value of $c^* = c_{\max}$ measured on day 2 for clarity. The correlation between ~~THAA and the normalized~~
378 ~~reduced~~ surfactant concentration c^*/c_{\max} and THAA was slightly higher ($r = 0.84$; $n = 7$; $p = 0.019$) than for
379 TCHO ($r = 0.79$; $n = 7$, $p = 0.034$). Together with the higher abundance of THAA and presumably higher surface
380 activity of polypeptides compared to polysaccharides (Burrows et al., 2014), this is another indication that, in
381 particular, protein-rich material was important for the formation of the highly surfactant-covered air-water
382 interface.

383

384 3.2 Sea surface properties and biochemical SML composition at increasing wind speed

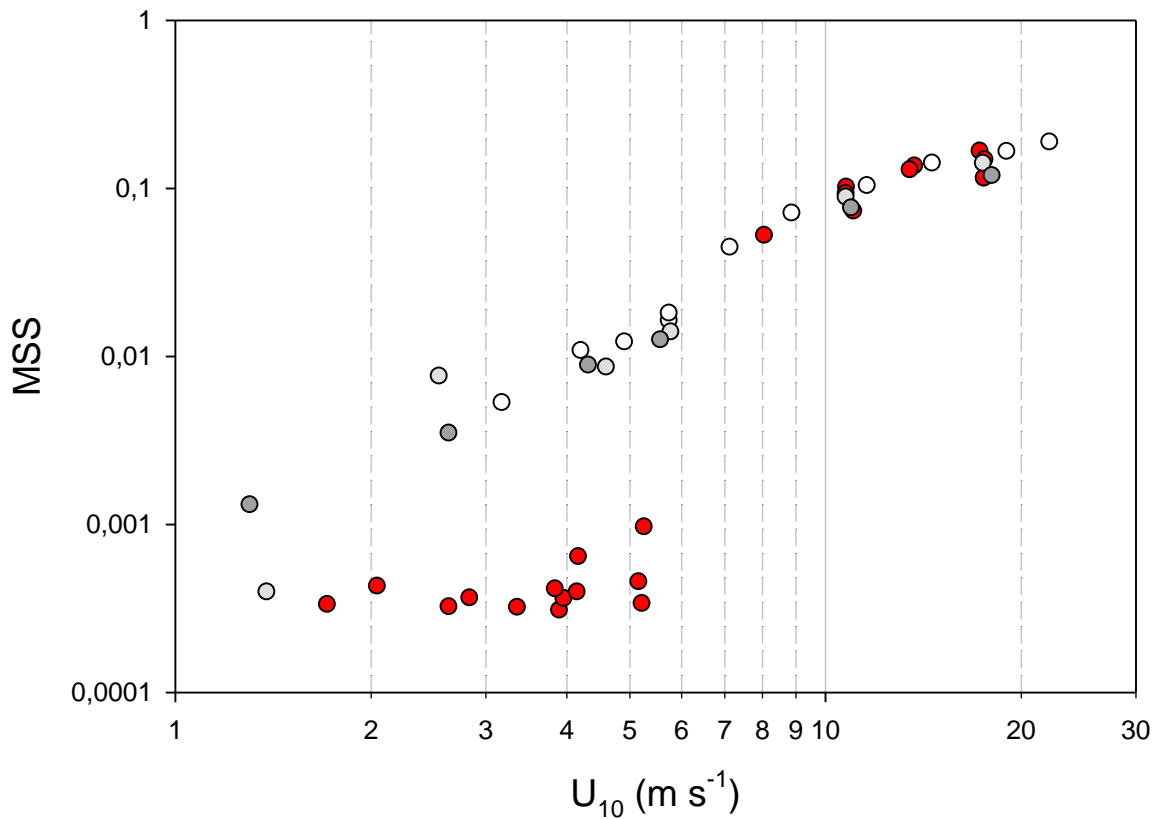
385 During the ~~Aeolotron~~Aeolotron study and all seven wind experiments, the water column was covered by an SML,
386 with an apparent thickness (d) of 31 - 50 μm . In the course of the *Aeolotron* experiment, SML thickness increased
387 from $d=36\mu\text{m}$ on day 2 to $d=45\mu\text{m}$ on day 24, determined at low wind speed for each measurement day.
388 Combining all data from wind speed experiments days 4 to 24 showed clear patterns regarding the relationship
389 between SML thickness and wind speed (Figure 3). Overall, d increased gradually and significantly with wind
390 speeds ($r=0.63$, $n=34$, $p < 0.001$). The value of d varied between the same wind speed of different experiments, but
391 was always lowest at low wind speeds, suggesting that SML disruption and mixing between the SML and ULW
392 and surface accumulation of organic components during high wind speeds had no long-lasting (~~i.e.~~($\geq 24\text{hrs}$), i.e.)
393 memory effects on SML thickness.

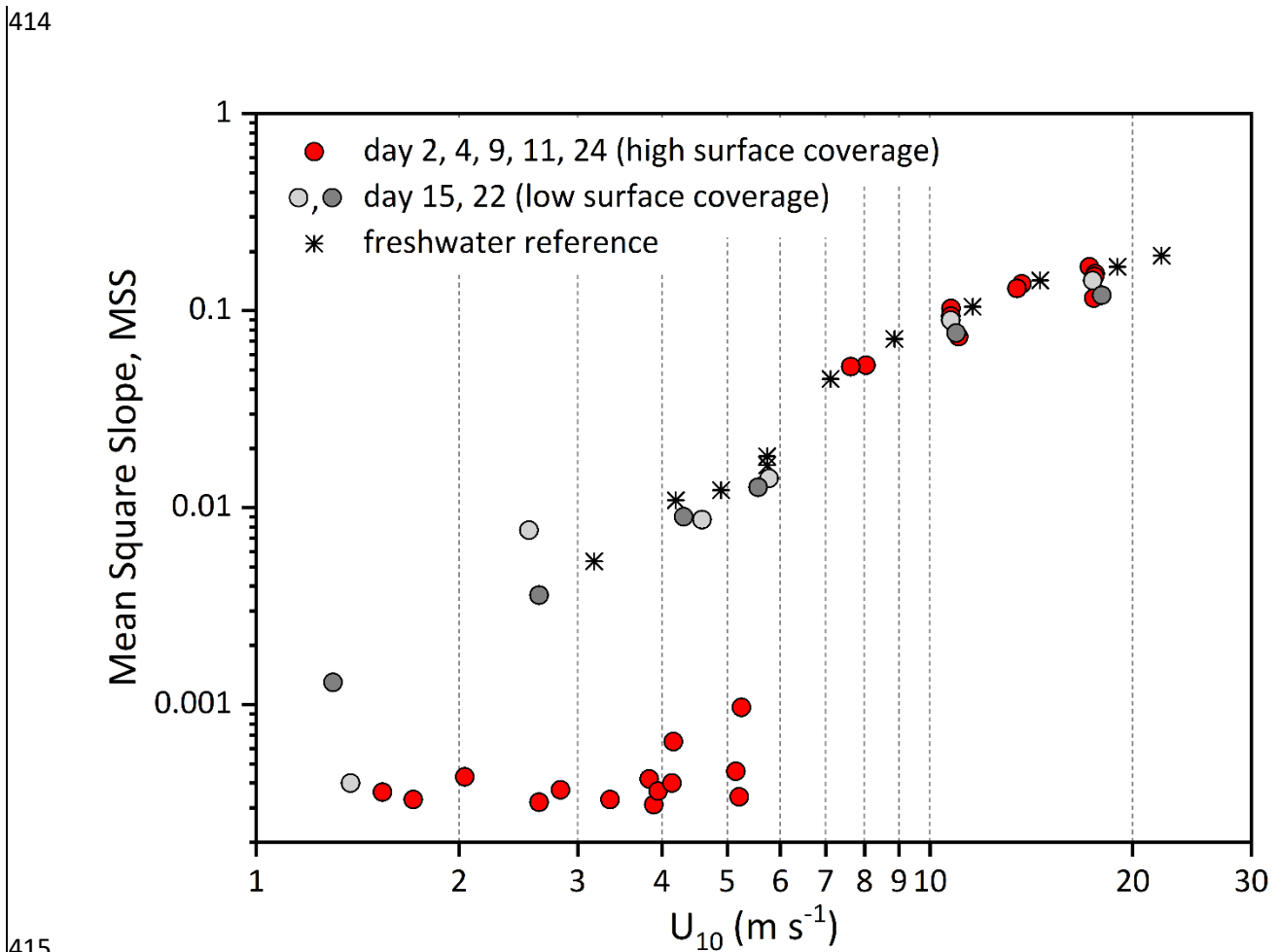


396 **Figure 3: Relationship between wind speed (U_{10}) and the apparent thickness of the SML (d) as assessed by**
397 **glass-plate sampling during the *Aeolotron* experiment.**

398

399 ~~The MSS value of the water surface was determined to measure surface roughness~~The surface roughness, a
400 ~~measure of the small- to medium-scale structure of the wave field that controls how the sea interacts with wind~~
401 ~~and light, has been determined by means of the MSS value~~, a parameter directly correlated with air-sea exchange
402 of gases and heat. Reference freshwater MSS values showed a gradual increase with wind speed (U_{10}) from
403 ~~5.31×10^{-3} to 1.91×10^{-1}~~ 5.31×10^{-3} at 3.2 m s^{-1} to 1.91×10^{-1} at 22.71 m s^{-1} (Figure 4). ~~The total range of MSS values for natural~~
404 ~~seawater was $3.0 \times 10^{-4} - 1.67 \times 10^{-1}$~~ . Compared to freshwater, MSS values abruptly changed around 6 m s^{-1} and
405 were about ~~one order~~1-2 orders of magnitude lower at wind speeds of $U_{10} < 6 \text{ m s}^{-1}$ during experiments conducted
406 on days 2, 4, 9, 11 and 24. ~~On days 15 and 22, This strong wave-damping effect at $U_{10} < 6 \text{ m s}^{-1}$ was accompanied~~
407 ~~by high surfactant surface coverage values of $sc > 0.74$. On days 15 and 22, with $sc < 0.47$, surface coverage was~~
408 ~~significantly lower, and the corresponding~~ MSS values at low windspeed were clearly higher and close to those
409 observed for freshwater, yielding values of 1.32×10^{-3} - 3.52×10^{-3} . At wind speeds $> 6 \text{ m s}^{-1}$, MSS generally
410 ~~increased~~continued to increase with wind speed ~~but showed~~for all available natural seawater samples and, despite
411 ~~some~~ variability between the experimental days ~~also~~. ~~The total range of MSS values for natural seawater was 3.0~~
412 ~~$\times 10^{-4} - 1.67 \times 10^{-1}$~~ , closely followed the freshwater trend.



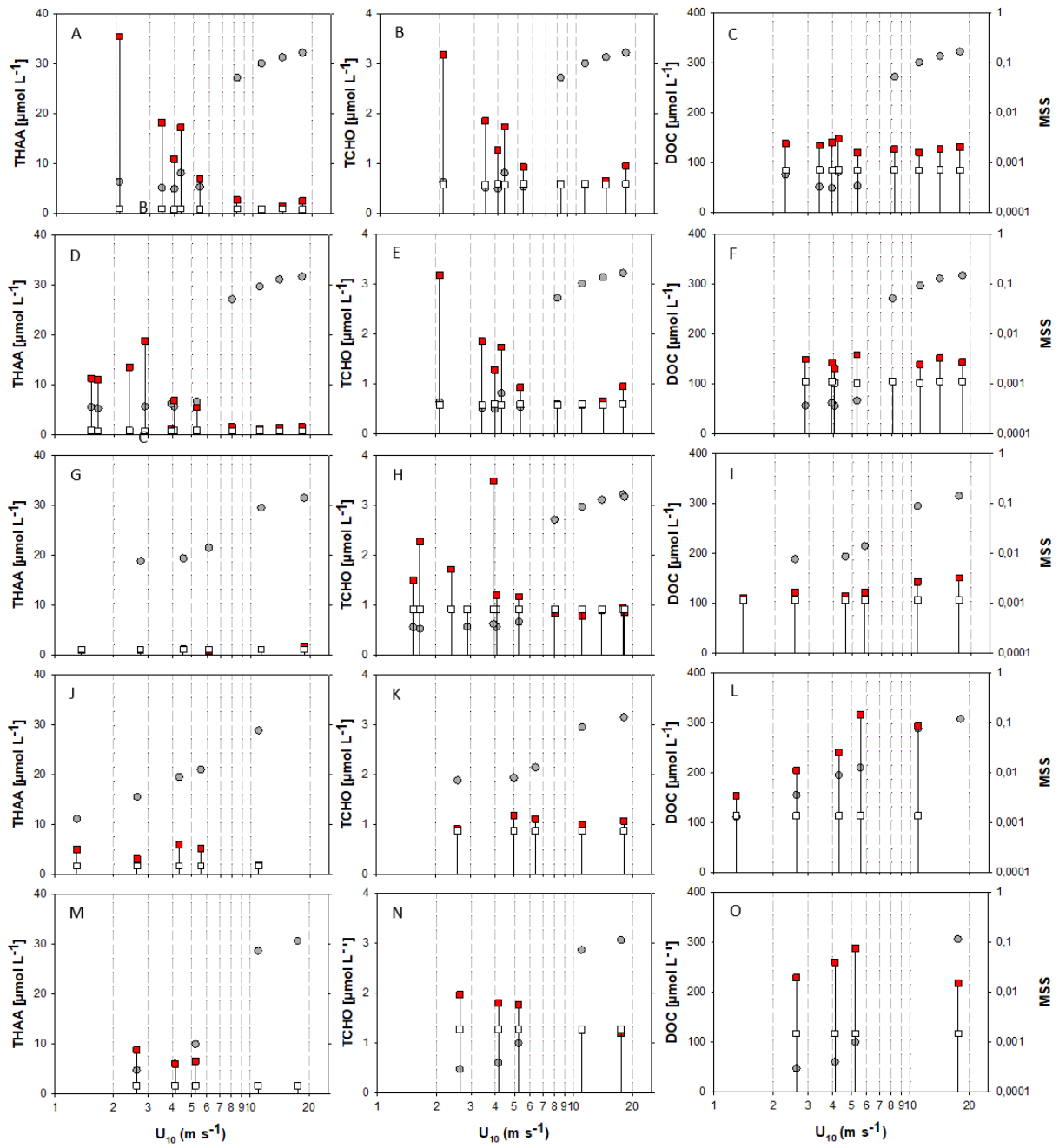


416 **Figure 4: Mean Square Slopes (MSS, dimensionless) relative to wind speed (U_{10} , $m s^{-1}$) during experiments**
 417 **with natural seawater. Days 2, 4, 9, 11 and 24 (red circles) with significant wave damping at wind speeds**
 418 **<6 $m s^{-1}$; day 15 (light grey circles), and day 22 (grey circles) with little wave damping compared to pure**
 419 **freshwater (open circles asterisk).**

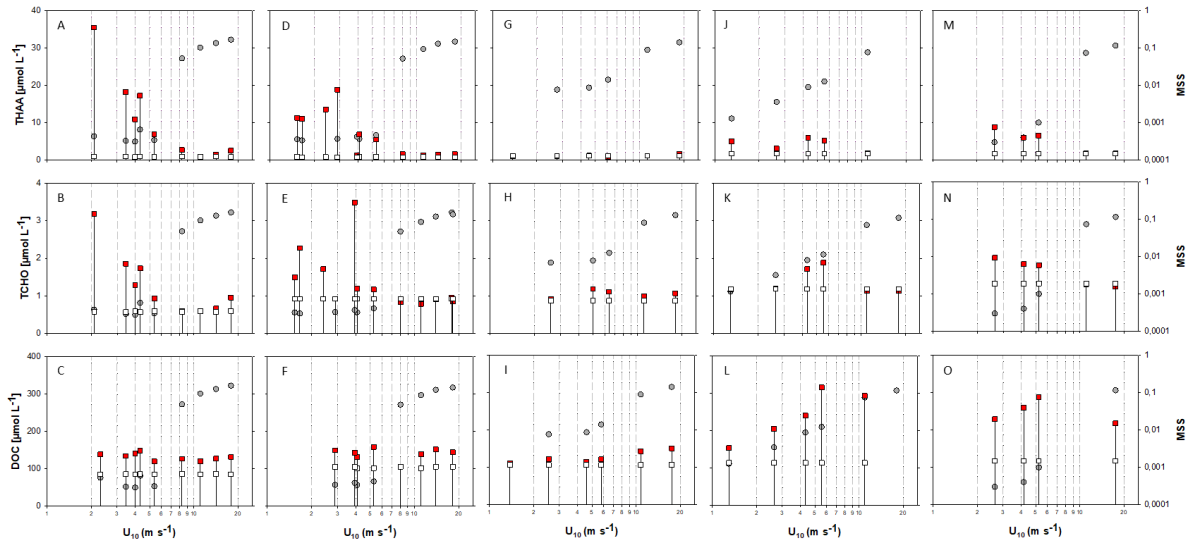
421 For a better representation of biopolymer accumulation in the SML at different wind speeds, we grouped data for
 422 days 2 and 4, and for days 9 and 11. Days 15, 22 and 24 showed different patterns and are shown individually. In
 423 accordance with previously observed enrichment patterns, concentrations of biopolymers in the SML declined
 424 with increasing wind speed, showing a pronounced step to lower values at wind speeds $> 5-6 m s^{-1}$. This effect
 425 was most evident for experiments days 2-11, having the highest initial SML biopolymer concentration (Figure 5A-
 426 O). At wind speed $>5-6 m s^{-1}$, THAA and TCHO concentrations in the SML were similar or equal to ULW
 427 concentration. This collapse of the biopolymeric SML enrichment coincided with the sudden and pronounced
 428 change in MSS. On day 15, biopolymer concentration in the SML was not different from the ULW at initially low

429 wind speed. The absence of an organic SML enrichment on day 15 may be attributed to enhanced microbial
430 decomposition and is supported by the amino-acid-based degradation index (DI), which was lowest on day 15,
431 suggesting a high degree of degradation (Engel et al., 2018). In this sense, the slight increase of DOC with
432 increasing wind speeds on day 15 and even more pronounced on days 22 and 24, i.e., after the addition of
433 phytoplankton and phytoplankton-derived organic matter to the ULW, suggests that organic matter of the
434 underlying water enriched the SML again, likely due to enhanced mixing and rising of film-covered bubbles after
435 wave-breaking ~~(Figure 5I)~~, which is an established mechanism discussed in literature (Blanchard, 1975; Stefan
436 and Szeri, 1999; Sabbaghzadeh et al., 2017) (Figure 5I). On days 22 and 24, higher biopolymer concentrations in
437 the SML were observed again, likely due to the addition of organic matter from a phytoplankton culture (day 20)
438 and slick material from an earlier mesocosm study (day 21). Biopolymer concentration and enrichment, however,
439 stayed below values observed during the first two weeks of the experiment. Enrichment of the biopolymers THAA
440 and TCHO in the SML ranged between 0.74 and 38 for EF_{THAA} and between 0.70 and 5.77 for EF_{TCHO} and fell to
441 values ~ 1 at $U_{10} > 5-6 \text{ m s}^{-1}$ also.

442 Enrichment of DOC in the SML varied between EF_{DOC} 1.04 and 2.78 and was not directly related to wind speed.
443 In contrast to THAA and TCHO, DOC concentration in the SML remained higher than in the underlying bulk
444 seawater or even increased at increasing wind speed. Differences in DOC concentrations between SML and bulk
445 seawater were moderate during experiments days 2, 4, 9 and 11 (Figure 5C, F), lowest on day 15 (Figure 5I) and
446 highest for the experiments conducted after the addition of organic material (Figure 5L, O).



447



448

449

450

451

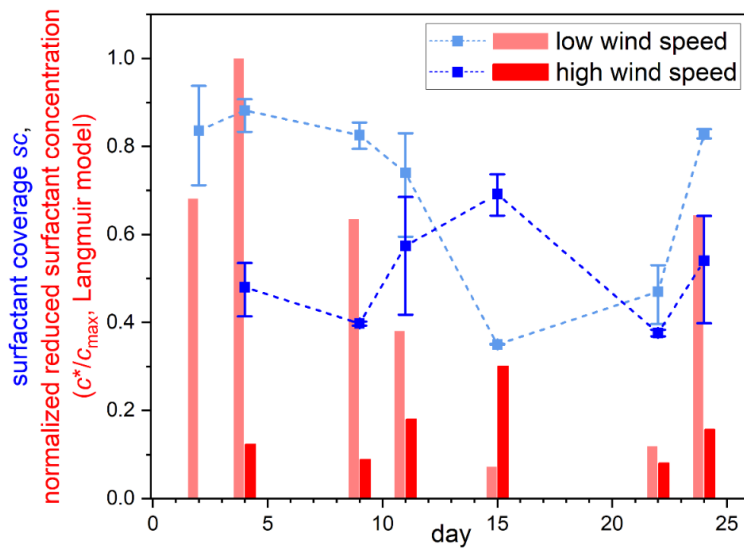
452

453

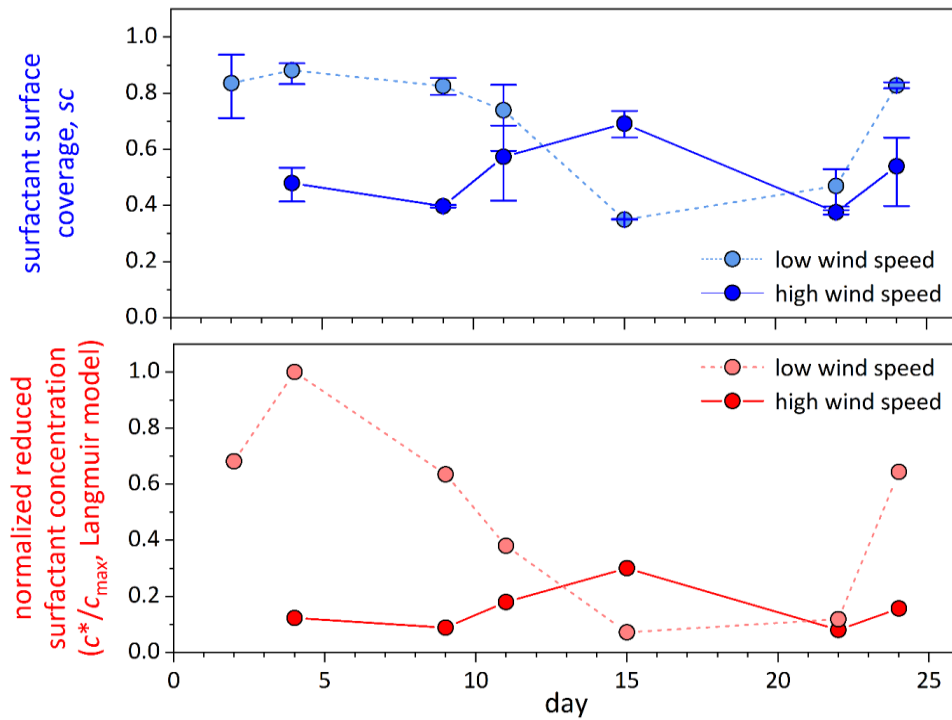
Figure 5A-O: Changes in organic matter components in the SML (red rectangles) and ULW (grey rectangles) at different wind speeds (U_{10}), and associated MSS values (grey circles). For better coverage of wind speeds, samples with similarities in SML biopolymer concentrations and surface coverage were pooled, specifically, samples were grouped for days 2 and 4: A-C and days 9 and 11: D-F. Day 15: G-I, day 22: J-L, day 24: M-O. Drop lines show associated SML-ULW pairs.

454

455 Surfactant surface coverage and the corresponding reduced surfactant concentration in the bulk SML were
456 determined only at the lowest and highest wind speeds, respectively (Figure 6). Both quantities were clearly
457 reduced at high wind speed, except for day 15. As already outlined above, in contrast to all other days, day 15 did
458 not show an enrichment of organics in the SML, along with a presumably high degree of degradation.
459 ~~There with~~Consequently, surfactant surface coverage closely resembled biopolymer accumulation in the SML. In
460 general (excluding day 15), surfactant surface coverage (factor 1.6 ± 0.2 , $n = 5$) and effective surfactant
461 concentration (factor 4.6 ± 1.5 , $n = 5$) were smaller at high wind speed and less variable at low wind speed,
462 supporting the idea of surfactant accumulation in slicks.



463



464

465 **Figure 6: Surfactant surface coverage sc (blue symbols) and normalized reduced bulk SML surfactant**
 466 **concentration c^*/c_{max} (bars), as determined by VSFG spectroscopy for SML samples at the end of the**
 467 **lowest (light color) and highest wind speed (dark color) setting. No surfactant data were obtained at high**
 468 **wind on day 2.**

469

470

471

472

473 **3.34 Wind-induced changes in biopolymer composition**

474 ~~Along with~~ In addition to concentration changes, wind speed, also altered the monomeric composition of
 475 biopolymers in the SML ~~changed~~. Wind speed clearly affected THAA composition in the SML, with a significant
 476 decrease in molar contributions of PHE, VAL, ARG, and ISO ($p < 0.001$) and significant increases ($p < 0.001$) in
 477 GLY, GABA, SER, and LEU, while changes were less or not significant for TYR, ALA, GLX, ASX, and THR
 478 (Table 1). At times of high THAA enrichment ($EF_{THAA} > 6$), i.e. days 2-11, a strong selective enrichment of ARG
 479 and GLX was observed in the SML at all wind speeds, with EF_{Arg} being approximately twice as high as EF_{THAA}

480 (Figure 7A). In contrast, GABA was relatively depleted in the SML, with EF_{GABA} being less than half as much as
481 EF_{THAA} . Selective enrichment of ARG vanished after day 15 and was only slightly higher on days 22 and 24, with
482 the highest $EF_{ARG}=6.8$ at $EF_{THAA}=5.3$.

483 Wind-induced changes in THAA composition indicate that the rather fresh organic material that accumulated at
484 the SML under low wind conditions was mixed into the underlying seawater and replaced at higher wind speeds
485 by more diagenetically altered material. This was evident from the DI index being systematically higher at wind
486 speed $<6 \text{ m s}^{-1}$ than above (Figure 1S). Again, only day 15 stood out of this pattern with similarly low DI indices
487 at all tested wind speeds.

488 In contrast to THAA, wind-induced effects on the carbohydrate composition of biopolymers were less
489 pronounced. A clearly significant selective decrease with increasing wind speed was observed for GLC-N, GAL
490 and RHA (Table 1). Also, GAL became depleted at increasing winds, while no impact was observed on the uronic
491 acids GLC-URA and GAL-URA, as well as on FUC. ARA was the only sugar that became clearly enriched in the
492 SML with increasing wind speed, while GLC and XYL/MAN, being quantitatively the most important sugars,
493 showed only a moderate relationship with wind speed.

494 Like individual amino acids, some sugars were selectively enriched in the SML, in particular when TCHO
495 enrichment was relatively high ($EF_{TCHO}>2$) (Fig. 7B). This was most pronounced for the amino-sugar GAL-N with
496 $EF_{GAL-N}:1.08-12.9$ compared to TCHO with $EF_{TCHO}:0.70-5.77$. Interestingly, only a slight selective enrichment
497 was observed for the two uronic acids determined during this study when compared to EF_{TCHO} , i.e. GAL-URA
498 ($EF_{GAL-URA}:0.51-6.57$) and GLC-URA ($EF_{GLC-URA}:1.04-6.57$). Uronic acids are building blocks of complex gel-
499 like colloidal and particulate material suggested to form the SML (Sieburth, 1983; Cunliffe and Murrell, 2009),
500 and accumulation of carbohydrate-rich gel-like transparent exopolymer particles (TEP) was also observed during
501 this study (Sun et al., 2018). ARA and XYL/MAN were consistently less enriched than TCHO, showing
502 $EF_{Ara}:0.44-3.12$ and $EF_{XYL/MAN}:0.41-3.55$, respectively.

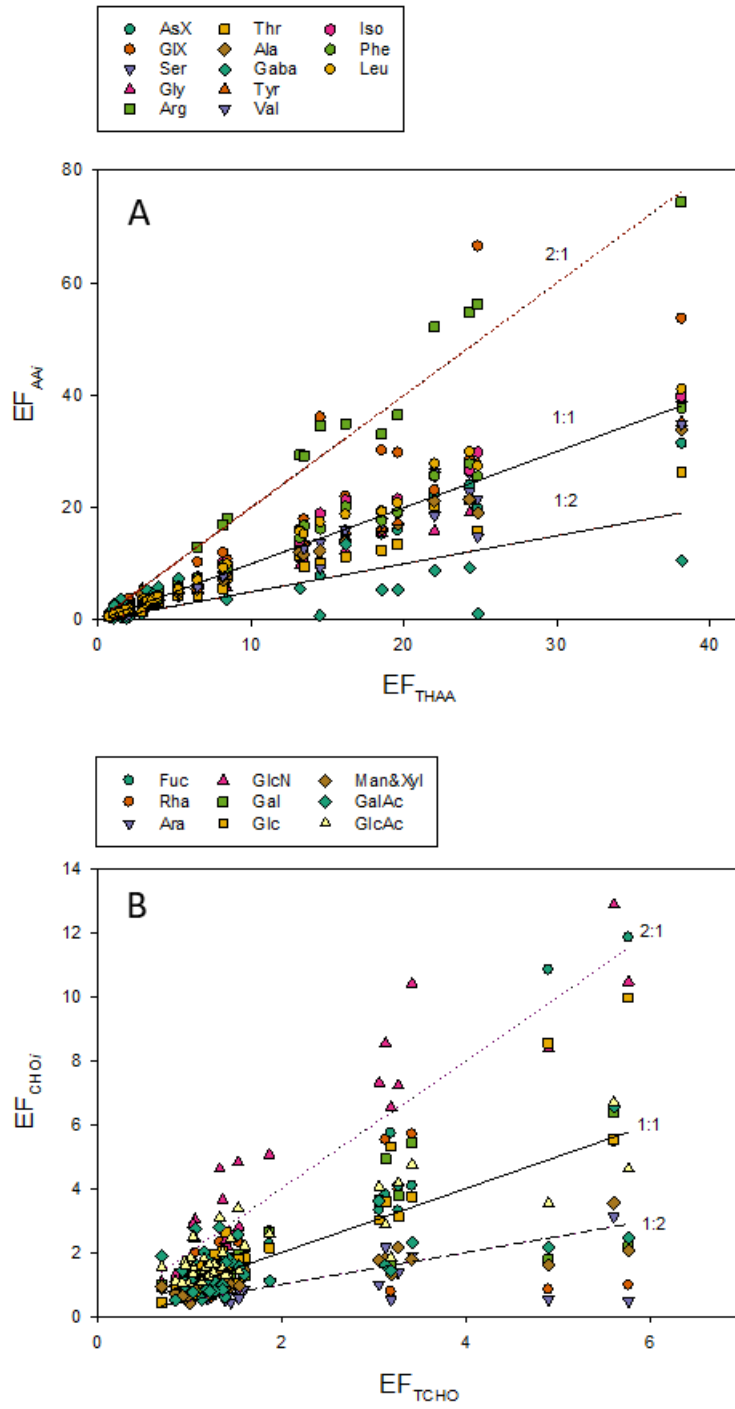
503

504

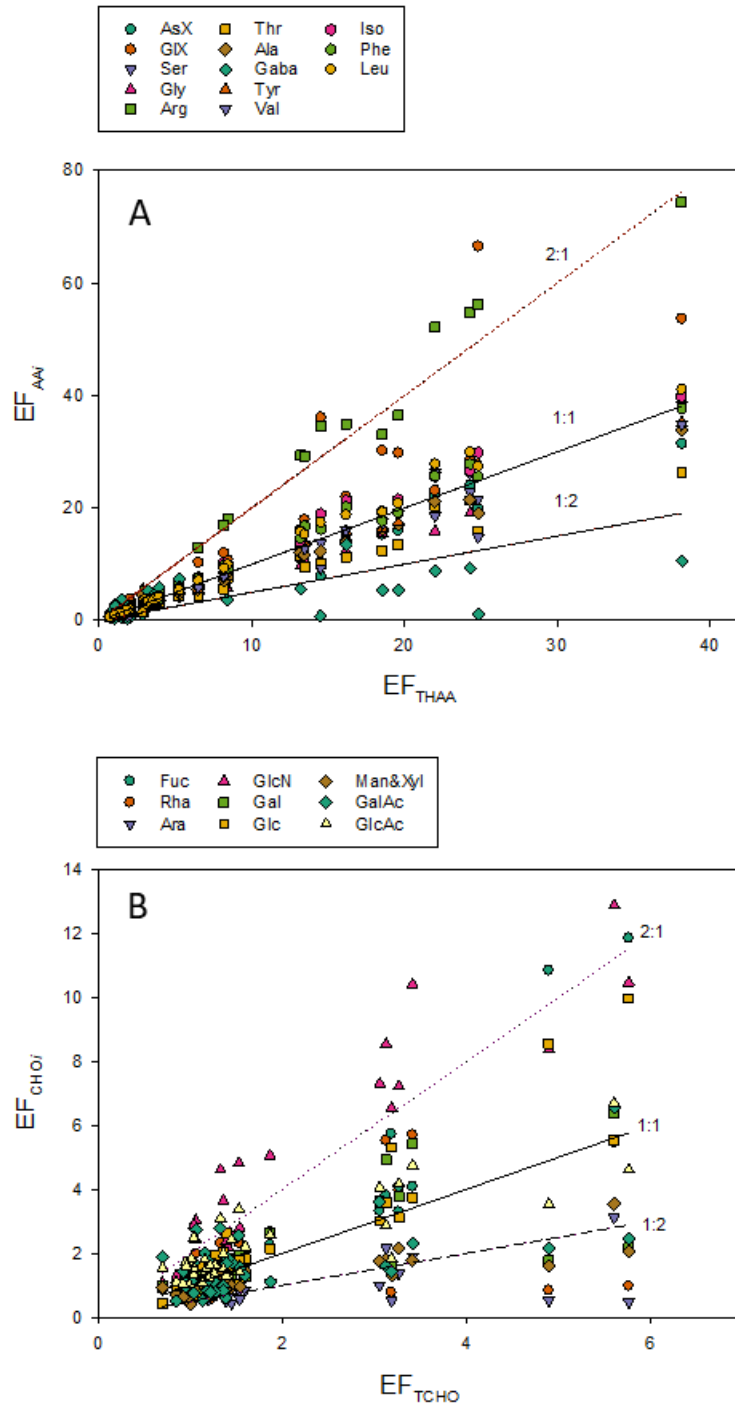
505

506 **Table 1: Correlation between wind speed (U_{10}) and monomeric components (Mol%) of TCHO (left column)**
507 **and THAA (right column) as observed for the SML samples. n.s.: not significant.**

	<i>r</i>	<i><p</i>		<i>r</i>	<i><p</i>
GLC-N	-0.761	0.001	PHE	-0.885	0.001
RHA	-0.687	0.005	VAL	-0.774	0.001
GAL	-0.425	0.01	ARG	-0.705	0.001
FUC	-0.216	n.s.	ISO	-0.675	0.005
GLC-URA	-0.197	n.s.	TYR	-0.389	0.01
GAL-URA	-0.077	n.s.	ALA	-0.34	0.01
GLC	0.419	0.01	GLX	-0.339	0.01
XYL/MAN	0.457	0.01	ASX	-0.203	n.s.
ARA	0.731	0.001	THR	0.0956	n.s.
			GLY	0.645	0.001
			GABA	0.674	0.001
			SER	0.712	0.001
			LEU	0.836	0.001



509



510

511 **Figure 7A, B: Relationships between Enrichment Factors (EFs) of individual amino acids (EF_{AAi}) and total**
512 **hydrolysable amino acids (EF_{THAA}) (A) and between EFs of individual sugars (EF_{CHOi}) and total combined**
513 **carbohydrates (EF_{TCHO}) (B). Lines shown for reference: 2-fold enrichment (2:1), no enrichment (1:1) and**
514 **2-fold depletion (1:2).**

515

516

517 4. Discussion

518 4.1 Accumulation of biopolymers at the air-sea interface

519 Seven experiments were conducted with natural seawater in the annular wind-wave channel *Aeolotron* and
520 revealed distinct patterns regarding the accumulation of natural organic matter in the SML, the impact of wind
521 speed on biopolymer enrichment and composition, as well as the effects of biopolymer enrichment on capillary
522 wave damping. Firstly, biopolymers, specifically substances containing amino acids and carbohydrates, were
523 found to be highly enriched in the SML at low wind speeds ($<6 \text{ m s}^{-1}$).

524 Biopolymers have long been considered important in the SML dynamics; the SML itself proposed to be a highly
525 hydrated loose gel of tangled macromolecules and colloids (Sieburth, 1983; Cunliffe and Murrell, 2009). During
526 this study, the range of biopolymer (THAA + TCHO) concentration in the SML was $1.4\text{-}40 \mu\text{mol L}^{-1}$, which is
527 comparable to the range observed in the ocean. For instance, average SML concentrations of $1.72 \pm 0.44 \mu\text{mol L}^{-1}$
528 TAA and $1.1 \pm 0.49 \mu\text{mol L}^{-1}$ TCHO were determined in the tropical Eastern North Atlantic (Barthelmeß et al.,
529 2021) and approximately $2 \mu\text{mol L}^{-1}$ THAA and $2.5\text{-}3.8 \mu\text{mol L}^{-1}$ TCHO were found in the western Baltic Sea
530 (Barthelmeß and Engel, 2022). In the highly productive upwelling system off Peru, SML concentrations can reach
531 up to $6 \mu\text{mol L}^{-1}$ THAA and $7.8 \mu\text{mol L}^{-1}$ TCHO (Engel and Galgani, 2016). For the North-Western Atlantic
532 Ocean, THAA concentrations of up to $10 \mu\text{mol L}^{-1}$ have been reported (Kuznetsova et al., 2004). Likewise, variable
533 and high enrichments of biopolymers in the SML have been observed. For instance, EFs of dissolved amino acids
534 varied between 5 and 43 in the subtropical Atlantic and Mediterranean Seas (Reinthal et al., 2008) and between
535 1.1 and 9 in the Eastern Tropical South Pacific⁵⁴-Pacific (Zäncker et al., 2017). As observed during this study, the
536 enrichment of amino acids in the SML often exceeds the enrichment in carbohydrates (Engel and Galgani, 2016;
537 Zäncker et al., 2017; van Pinxteren et al., 2012).

538 Based upon high biopolymer enrichment, the SML often shows typical biofilm properties (Wurl and Homes,
539 2008), with high biological activity and specifically adapted organisms, i.e., neuston. Hydrolysis experiments
540 revealed that microbial activity can significantly reduce amino acid concentrations in microlayer samples, even to
541 values below those found in the underlying water (Kuznetsova and Lee, 2001). During this study, the amino acid
542 and carbohydrate concentrations in the SML were reduced to the ULW level by day 15, indicating that microbial
543 degradation may indeed counteract biopolymer accumulation and, therefore, slick formation in the sea.

544

545 4.2 Interactions of wind speed and biopolymer accumulation in the SML

546 The conditions in the *Aeolotron* at low wind speeds resembled typical slick conditions as observed in the field.
547 The most prominent property of surfactants is their damping of capillary waves, as indicated by a reduction in the
548 MSS value. The damping effect results from the dissipation of wave energy due to changes in the viscoelasticity
549 of the interfacial surface layer (Cini et al., 1983) and is referred to as the Marangoni effect (McKenna and Bock,
550 2006). The intensity of the Marangoni effect depends on the quantity and composition of surface-active compounds
551 in slicks. Under slick conditions, accompanied ~~with~~by high values of surfactant coverage, MSS values in the
552 *Aeolotron* were reduced by ~~one order~~about 1-2 orders of magnitude compared to ~~clear~~the freshwater reference.
553 However, the damping effect largely vanished at $>6 \text{ m s}^{-1}$ ~~when~~. At a wind-speed threshold of approximately 6 m
554 s^{-1} , the collapse of the biopolymeric SML—collapsed surface layer induced an abrupt change in sea-surface
555 roughness. Because the MSS is widely recognized as a predictor of air–sea gas transfer velocity (McKenna and
556 Bock, 2006; Frew et al., 2004), such an abrupt shift in surface roughness should likewise be reflected in the gas-
557 transfer measurements. Indeed, Ribas-Ribas et al. (2018) reported a decrease in N_2O gas transfer velocities at wind
558 speeds of approximately $U_{10} = 5.5\text{--}8 \text{ m s}^{-1}$, during an accompanying *Aeolotron* experiment—findings that are
559 highly consistent with our observations.

560 Previous wind-wave tank experiments, not carried out on natural samples but with strong artificial surfactants,
561 showed significant wave damping until wind speeds of $U_{10} \sim 18 \text{ m s}^{-1}$ (Alpers and Hühnerfuss, 1989). During
562 experiments in a linear wind-wave tunnel, an artificial surface film (oleyl alcohol) began to tear at a wind speed
563 of 13 m/s (Broecker et al., 1978). Previous *Aeolotron* experiments with surface films of hexadecanol and olive oil
564 and with the soluble surfactants Triton X-100 and Tergitol 15-S-12 at a concentration of 5 ppm also showed
565 damping effects at higher wind speed (Jähne, *unpublished*). So far, wind-wave tank experiments with natural
566 seawater and, hence, natural surfactants and surface films remain scarce. Our data show that the wave-damping
567 effects of biogenic surface films may behave differently from artificial films. Natural SML components may be
568 more susceptible to wind-induced disruption and more variable over time and space. Biopolymer variability in the
569 SML may thus be expected over the diurnal cycle, as wind speed often increases during the night. Our data also
570 show that the amount and chemical composition of biopolymers and, in consequence, the surface activity can vary
571 with microbial production and decomposition. Due to natural chemical heterogeneity, the impact of natural surface
572 film on air-sea gas exchange, however, may differ from our observations ~~when~~. In particular, where stronger
573 surfactants are ~~included that~~present, also natural films may resist higher wind speeds. For instance, surfactant
574 enrichment in the SML has been reported for wind speeds of up to 9.5 m s^{-1} (Wurl et al., 2011); DOC enrichment

575 up to 9.7 m s^{-1} in the Mediterranean Sea (Reinthal et al., 2008), and enrichment of combined amino acids in the
576 North Atlantic Ocean at wind speeds of 7 m s^{-1} (Kuznetsova et al., 2004). Clearly, a mechanistic understanding of
577 wind speed and SML biopolymer enrichment has yet to be established. In this regard, conducting controlled wind-
578 wave experiments using natural seawater can offer important insights into the role of natural surfactants in
579 modulating air-sea gas exchange.

580 On the one hand and in contrast to THAA and TCHO biopolymers, no significant relationship between wind speed
581 and DOC enrichment was observed. On the other hand, the apparent thickness of the SML increased significantly
582 with rising wind speeds. The sensitivity of SML thickness to wind speed has been reported previously, with an
583 increase in apparent SML thickness up to wind speeds between 5.5 and 7.9 m s^{-1} (Beaufort 4) in the Baltic Sea
584 (Falkowska, 1999), or a decrease in SML thickness with wind speeds ranging from 1 to 5 m s^{-1} (Liu and Dickhut,
585 1998). This may be explained by different and partly antagonistic processes influencing organic matter enrichment
586 in the SML. On the one hand, wind can reduce microlayer enrichment through turbulent mixing, which increases
587 with wind speed. Conversely, wind can enhance the enrichment of certain components by promoting bubble
588 formation, which facilitates the scavenging of organic matter from the ULW to the microlayer (Hunter and Liss,
589 1981). In the environment, other processes also interact with organic matter enrichment, such as the production or
590 decomposition of organic matter in the SML or the mixing and advection of water masses. Our study allowed us
591 to follow the changes in SML composition with increasing wind speed and suggests that the enrichment of organic
592 matter in the SML and its response to wind is highly compound-specific. Biopolymers, i.e. TCAA and TCHO,
593 showed the highest EFs and responded similarly to increasing wind, with no discernible difference between SML
594 and underwater concentrations at wind speed $> 6 \text{ m s}^{-1}$. DOC is a bulk measure and includes a variety of different
595 substances that may be more or less prone to mixing or enrichment. Indeed, EFs for DOC were rather low
596 compared to THAA and TCHO. DOC concentration in the SML may ~~be~~ simply be high because of diffusive
597 exchange with high background concentration of organic substances do not have surfactant properties. Hence, a
598 uniform relationship of DOC enrichment in the SML with regard to wind speed seems unlikely. In this study, DOC
599 concentration and enrichment in the SML increased with wind speed on day 15 and were even more pronounced
600 on days 22 and 24. This indicates a net upward transport of DOC from the ULW to the SML due to increased
601 turbulence or rising bubbles at higher wind ~~speeds~~speeds. Because of the high concentration of DOC, an increase
602 in DOC may have contributed to the increase in apparent thickness (d) of the SML with wind speed observed
603 during this study, although it cannot fully explain it. This also shows that apparent SML thickness and visually
604 apparent slick conditions are not necessarily related.

605 During the first two weeks in the *Aeolotron*, slicks showed THAA accumulation up to 10 times higher than TCHO
606 accumulation. This aligns with observations that protein-rich, gel-like particles were highly enriched at low wind
607 speeds, especially in the early stages of the experiment (Sun et al., 2018). At the same time, the highest surfactant
608 coverage, as determined by VSFG-spectroscopy, was observed. The [THAA]:[TCHO] or, more generally, the
609 protein/carbohydrate (P/C) ratio in the SML was highest on days 2 and 4. This suggests that polypeptides not only
610 played an important role in slick formation but also included particularly powerful biosurfactants. The P/C ratio
611 of biopolymers has been interpreted as an indicator for the relative hydrophobicity of extracellular polymeric
612 substances (EPS) (Santschi et al., 2020), based on observations of increasing hydrophobic contact area (HCA)
613 with increasing P/C ratio (Xu et al., 2011). Exopolymers with high P/C ratios are mainly produced by bacteria,
614 whereas phytoplankton EPS contain more carbohydrates (Santschi et al., 2020). The high P/C ratio of surface
615 slicks at the beginning of this study can be explained by the predominance of bacterial biomass in the seawater,
616 which was collected in the deep North Sea and not exposed to light until day 8 of the experiment. Our observations
617 showed that capillary waves were most strongly damped on days 2-11. In contrast, the P/C ~~ratio~~ ratio was much
618 lower, with values ~4, when SML material from phytoplankton origin replenished the organic matter pool of the
619 SML on days 22 and 24. Since the seawater, which was used ~~for~~ to fill the *Aeolotron*, had been stored in the dark
620 for ~~more than two months~~ about one month prior to the experiment, any fresh material must have been derived
621 mainly from heterotrophic ~~mainly~~ bacterial production. The high P/C ratio, together with the high DI value of the
622 organic material in the SML at the beginning of the study, suggests that bacterial-derived biopolymers accumulate
623 and act as powerful biosurfactants in the SML.

624 Within the pool of THAA and THCO, monomers with ~~di-electric~~ dielectric properties (basic/acidic AAs and
625 basic/acidic CHO) were most enriched and most sensitive to wind speed, suggesting that surfactant properties are
626 linked to those monomeric components. Among the amino acids, significantly enriched in the SML were GLX
627 and ARG. High GLX and ARG enrichment has been reported for oceanic SML previously (Barthelmeß et al.,
628 2021; Sun et al., 2018; van Pinxteren et al., 2012). In general, the enrichment of amino acids at the air-sea interface
629 depends on their amphiphilic properties (Ćosović and Vojvodić, 1998), which arise from the degree of polarity
630 exhibited on their molecular surfaces. Among the amino acids discussed here, ARG and GLX are considered
631 hyperpolar and represent typical hydrophilic head groups of biosurfactants. Lipoamino acids derived from ARG
632 have increasingly gathered interest in biotechnological applications as they represent nontoxic and degradable
633 cationic biosurfactants with anti-microbial properties (Singh and Tyagi, 2014). Surfactant activity in surface waters
634 of the Tropical Eastern North Atlantic has been directly related to ARG concentration (Barthelmeß et al., 2011).

635 The GLX-containing lipopeptide *Surfactin*, produced by *Bacillus spp.*, a species also found in seawater, is one of
636 the most effective biosurfactants (Zhen et al., 2023). During this study, we didn't identify the molecular structure
637 of surfactants. However, the high THAA enrichment in the SML, together with even higher selective enrichment
638 of ARG and GLX, and strong surfactant activity, point to lipoamino acids with a bacterial source during the first
639 days of this study.

640 Enrichment in the SML was generally smaller for TCHO than for THAA. On day 22, after material from a
641 phytoplankton culture and bloom experiment ~~were~~was added, and the P/C ratio in the SML decreased, MSS values
642 at comparable wind speeds were higher. Marine photoautotrophic plankton is the major source of biomolecules in
643 the ocean, providing ~50 Gt of organic carbon yr⁻¹. In general, the biochemical composition of autotrophic cells
644 comprises the following major components by weight: proteins (17–57%), carbohydrates (4.1–37%), and lipids
645 (2.9–18%) (Parsons et al., 1961). Extracellular polymers released from the autotrophic cell, however, contain
646 largely polysaccharides (Engel et al., 2004; Thornton, 2014). Among the carbohydrates that showed a selective
647 enrichment in the SML was FUC, a sugar that is typically found in polysaccharides released from phytoplankton
648 and seaweeds (Buck-Wiese et al., 2023), and GLC-N, a sugar contained in bacterial exopolymers (Maßmig et al.,
649 2024). GLC-N, RHA and Gal were particularly sensitive to wind speed. GLC-N is often contained in biosurfactants
650 and, like arginine, has received attention in the biotechnological search for replacement of toxic synthetic
651 surfactants. Rhamnolipids are typical biosurfactants consisting of one or two rhamnose sugar molecules linked to
652 hydroxy fatty acid chains. Galactolipids can be found in some cyanobacteria and algae and include galactose
653 residues linked to lipid moieties. However, compared to peptide-based surfactants, carbohydrate-based surfactants
654 seem to be less abundant or less effective during this study.

655 The amino-acids-based DI, as well as the presence of FUC, suggested that organic matter accumulating at the SML
656 was less degraded than in the underlying seawater. This finding ~~agrees well~~is consistent with earlier findings on
657 SML biopolymer composition and surfactant activity in the Baltic Sea (Barthelmess and Engel, 2022),
658 ~~showing which show~~ that the highest surface activity was triggered by the microbial release of fresh organic matter.
659 Marine microorganisms release surfactants for several ecological and physiological reasons. For example, they act
660 as emulsifiers and aid in substrate uptake, in particular hydrophobic organic compounds, such as oil, and are
661 produced by a variety of marine bacteria (Floris et al., 2020). Moreover, surfactants facilitate the colonization of
662 surfaces by helping microorganisms adhere to substrates and form biofilms. In higher organisms, e.g., mammals,
663 surfactants are critical to maintaining lung function or for skin protection. A common feature of surfactants is their
664 accumulation at interfaces. The air-sea interface, including both the SML and bubbles, represents the largest

665 interface in the ocean and serves as a trap ~~effor~~ surfactants released to seawater. Since microbial surfactants are
666 used extracellularly, they must be stable enough in the marine environment to fulfil their ecological roles. The
667 production and subsequent accumulation of biopolymers, including surfactants, in the SML illustrate how marine
668 life can alter the physical environment at the ocean's surface. This biotic effect on upper ocean physics has direct
669 implications for climate regulation, as changes in gas exchange and surface turbulence can impact the ocean's role
670 in sequestering carbon dioxide and regulating atmospheric gases. Thus, these effects may be particularly
671 pronounced in areas of high surfactant productivity, highlighting the complex interplay and feedback between
672 biodiversity, chemical diversity, and air-sea exchange in the ocean.

673

674 5. Conclusion

675 Our research revealed that biopolymers, particularly polypeptides, produced by marine microorganisms, serve as
676 efficient natural surfactants in the SML. Natural ~~polypeptides~~ surfactants that accumulated in the SML during this
677 study exhibited a significant damping effect on wave formation ~~as wind velocity increases up to wind speeds of~~
678 $U_{10} \approx 6 \text{ m s}^{-1}$. However, at even higher wind speeds and going along with the collapse of the biopolymeric SML,
679 the damping effect largely vanished. This sheds light on the ecological role of marine biopolymers and underscores
680 their influence on physical air-sea exchange processes. A better understanding of the dynamic linkages between
681 marine life and gas exchange could be pivotal to accurately assessing the ocean's present and future contributions
682 to the climate system, including the uptake or release of climate-relevant gases like CO₂ and methane.

683 5. Author contribution

684 AE conceptualized the study and provided the biopolymer data. GF provided the surfactant data. KK and BJ
685 contributed the MSS data. AE wrote the original manuscript. GF, KK, and BJ reviewed and edited the original
686 manuscript.

687 6. Data availability

688 The data supporting the findings of this study will be published on the PANGAEA data repository.

689 7. Competing interests

690 The contact author has declared that none of the authors has any competing interests.

691

692 **8. Acknowledgements:**

693 We thank the captain and crew of R/V POSEIDON and Armin Form for seawater collection. Thanks also go to
694 Martin Sperling and Cuici Sun for sampling the SML and underlying water during the *Aeolotron* experiment.
695 Kristian Laß is acknowledged for making available the VSFG data through the project CP1212 of the Kiel cluster
696 of excellence, “The Future Ocean”. Jon Roa, Ruth Flerus, Katja Laß and Tania Klüver are greatly acknowledged
697 for their technical support. We also thank Maximilian Bopp for providing friction velocity data. This work was
698 supported by the BMBF project SOPRAN III (Surface Ocean Processes in the Anthropocene 03F0662A-TP2.2)
699 and is a contribution to the international Surface Ocean Lower Atmosphere Study (SOLAS) and the DFG research
700 group Biogeochemical processes and Air–sea exchange in the Sea-Surface microlayer [BASS] SP1.1 ~~Dynamic~~
701 ~~enrichment processes of organic matter in the SML~~ Dynamic enrichment processes of organic matter in the SML
702 and 1.4 Chemical and photochemical transformation of organic matter.

703

704

705

706

707 **9. References:**

708 Alpers, W., and Hühnerfuss, H. (1989): The damping of ocean waves by surface films: A new look at an old
709 problem. *Journal of Geophysical Research*, *J. Geophys. Res.-Oceans*, 94, C5, 6251–6265, 1989.

710 Asher, W. E., Karle, L. M., and Higgins, B. J. (1997): On the differences between bubble-mediated air–water
711 transfer in freshwater and seawater. *Journal of Marine Research*, *J. Mar. Res.*, 55(5), 813–845, 1997.

712 Barthelmeß, T., Schütte, F., and Engel, A. (2021): Variability of the sea surface microlayer across a filament’s
713 edge and potential influences on gas exchange. *Frontiers in Marine Science*, 8, 718384, *Front. Mar. Sci.*, 8,
714 718384, <https://doi.org/10.3389/fmars.2021.718384>, 2021.

715 Barthelmeß, T., and Engel, A. (2022): How biogenic polymers control surfactant dynamics in the surface
716 microlayer: insights from a coastal Baltic Sea study. *Biogeosciences*, 19(20), 4965–4992,
717 <https://doi.org/10.5194/bg-19-4965-2022>, 2022.

718 Blanchard, D. C.: Bubble scavenging and the water-to-air transfer of organic material in the sea, in: *Applied*
719 *Chemistry at Protein Interfaces*, ACS Symp. Ser., 18, 360–387, American Chemical Society, 1975.

720 Bopp, M. (2014): Luft- und wasserseitige Strömungsverhältnisse im ringförmigen Heidelberger Wind-Wellen-
721 Kanal (Aeolotron), Master’s ~~Master’s~~ thesis, Institut für Umweltphysik, ~~Institut für Umweltphysik~~, Universität Heidelberg, Germany, DOI: <https://doi.org/10.11588/heidok.00017151>, 2014.

722 Broecker, H. C., Petermann, J., and Siems, W. (1978): The influence of wind on ~~CO₂~~ CO₂ exchange in a wind-
723 wave tunnel, including the effects of monolayers, *J. Mar. Res.*, 36, 595–610, 1978.

- 725 Buck-Wiese, H., Andskog, M. A., Nguyen, N. P., Bligh, M., Asmala, E., Vidal-Melgosa, S., ...and Hehemann, J.
726 H. (2023).: Fucoid brown algae inject fucoidan carbon into the ocean. *Proceedings of the National Academy of*
727 *Sciences*, Proc. Natl. Acad. Sci. USA, 120(4), e2210561119, <https://doi.org/10.1073/pnas.2210561119>, 2023.
- 728 Burrows, S. M., Ogunro, O., Frossard, A. A., Russell, L. M., Rasch, P. J., and Elliott, S. M. (2014).: A
729 physically based framework for modeling the organic fractionation of sea spray aerosol from bubble film
730 Langmuir equilibria. *Atmospheric Chemistry and Physics*, Atmos. Chem. Phys., 14(24), 13601–13629,
731 <https://doi.org/10.5194/acp-14-13601-2014>, 2014.
- 732 Cini, R., Lombardini, P. P., and Hühnerfuss, H. (1983).: Remote sensing of marine slicks utilizing their
733 influence on wave spectra. *International Journal of, Int. J. Remote Sensing, Sens.*, 4(1), 101–110, 1983.
- 734 Čosović, B., and Vojvodić, V. (1998).: Voltammetric analysis of surface active substances in natural seawater.
735 *Electroanalysis: An International Journal Devoted to Fundamental and Practical Aspects of*, Electroanalysis,
736 10(6), 429–434, 1998.
- 737 Croot, P. L., Passow, U., Assmy, P., Jansen, S., and Strass, V. H. (2007).: Surface active substances in the upper
738 water column during a Southern Ocean Iron Fertilization Experiment (EIFEX). *Geophysical Research Letters*,
739 34(3), Geophys. Res. Lett., 34, L03612, <https://doi.org/10.1029/2006GL028080>, 2007.
- 740 Cunliffe, M., and Murrell, J. C. (2009).: The sea-surface microlayer is a gelatinous biofilm. *The ISME*
741 *Journal*, 3(9), 1001–1003, <https://doi.org/10.1038/ismej.2009.69>, 2009.
- 742 Cunliffe, M., Engel, A., Frka, S., Gašparović, B., Guitart, C., Murrell, J. C., ...and Wurl, O. (2013).: Sea surface
743 microlayers: A unified physicochemical and biological perspective of the air–ocean interface. *Progress in*
744 *Oceanography*, Prog. Oceanogr., 109, 104–116, 2013.
- 745 Cunliffe, M., and Wurl, O. (2014).: Guide to best practices to study the ocean's surface, *Occas. Publ.*
746 *Mar. Biol. Assoc. UK*, 2014.
- 747 Cuscov, M., and Muller, F. L. (2015).: Differentiating humic and algal surface active substances in coastal
748 waters by their pH-dependent adsorption behaviour. *Marine Chemistry*, Mar. Chem., 174, 35–45, 2015.
- 749 Dauwe, B., and Middelburg, J. J. (1998).: Amino acids and hexosamines as indicators of organic matter
750 degradation state in North Sea sediments. *Limnology and Oceanography*, Limnol. Oceanogr., 43(5), 782–798,
751 1998.
- 752 Dauwe, B., Middelburg, J. J., Herman, P. M. J., and Heip, C. H. (1999).: Linking diagenetic alteration of
753 amino acids and bulk organic matter reactivity. *Limnology and Oceanography*, Limnol. Oceanogr., 44(7),
754 1809–1814, 1999.
- 755 Dittmar, T., Cherrier, J., and Ludwichowski, K. U. (2009).: The analysis of amino acids in seawater. *In, in:*
756 *Practical guidelines Guidelines for the analysis Analysis of seawater (pp. 79–90). Seawater*, CRC Press, 79–90,
757 2009.
- 758 Engel, A., Delille, B., Jacquet, S., Riebesell, U., Rochelle-Newall, E., Terbrüggen, A., and Zondervan, I.
759 (2004).: Transparent exopolymer particles and dissolved organic carbon production by *Emiliania huxleyi*
760 exposed to different CO₂ concentrations: a mesocosm experiment. *Aquatic Microbial Ecology*, Aquat.
761 *Microb. Ecol.*, 34(1), 93–104, 2004.
- 762 Engel, A., and Händel, N. (2011).: A novel protocol for determining the concentration and composition of
763 sugars in particulate and in high molecular weight dissolved organic matter (HMW-DOM) in seawater. *Marine*
764 *Chemistry*, Mar. Chem., 127(1–4), 180–191, 2011.
- 765 Engel, A., Harlay, J., Piontek, J., and Chou, L. (2012).: Contribution of combined carbohydrates to dissolved
766 and particulate organic carbon after the spring bloom in the northern Bay of Biscay (North Eastern Atlantic
767 Ocean). *Continental, Cont. Shelf Research, Res.*, 45, 42–53, 2012.

- 768 Engel, A., and Galgani, L. (2016). The organic sea-surface microlayer in the upwelling region off the coast of
769 Peru and potential implications for air-sea exchange processes. *Biogeosciences*, 13(4), 989–1007.
770 *Biogeosciences*, 13, 989–1007, <https://doi.org/10.5194/bg-13-989-2016>, 2016
771 Engel, A., Bange, H. W., Cunliffe, M., Burrows, S. M., Friedrichs, G., Galgani, L., ... and Zäncker, B. (2017). The ocean's vital skin: Toward an
772 integrated understanding of the sea surface microlayer. *Frontiers in Marine Science*, 4, 165.
- 773 Engel, A., Bange, H. W., Cunliffe, M., Burrows, S. M., Friedrichs, G., Galgani, L., and Zäncker, B.: The ocean's
774 vital skin: Toward an integrated understanding of the sea surface microlayer, *Front. Mar. Sci.*, 4, 165,
775 <https://doi.org/10.3389/fmars.2017.00165>, 2017.
- 776 Engel, A., Sperling, M., Sun, C., Grosse, J., and Friedrichs, G. (2018). Organic matter in the surface
777 microlayer: Insights from a wind wave channel experiment. *Frontiers in Marine Science*, *Front. Mar. Sci.*, 5,
778 182, <https://doi.org/10.3389/fmars.2018.00182>, 2018.
- 779 Edson, J. B., Jampana, V., Weller, R. A., Bigorre, S. P., Plueddemann, A. J., Fairall, C. W., Miller, S. D., Mahrt,
780 L., Vickers, D., and Hersbach, H. (2013). On the exchange of momentum over the open ocean. *Journal of*
781 *Physical Oceanography*, *J. Phys. Oceanogr.*, 43, 1589–1610, <https://doi.org/10.1175/JPO-D-12-0173.1>, 2013.
- 782 Falkowska, L. (1999). Sea surface microlayer: a field evaluation of ~~teflon~~ Teflon plate, glass plate and screen
783 sampling techniques. Part 1. Thickness of microlayer samples and relation to wind speed. *Oceanologia*, 41, 211–
784 221, 1999.
- 785 Floris, R., Rizzo, C., and Giudice, A. L. (2020). Biosurfactants from *Marine-marine metabolomics: new*
786 *insights into biology and medicine*. *Metabolomics: New Insights into Biology and Medicine*, 3, 2020.
- 787 Frew, N. M., Goldman, J. C., Dennett, M. R., and Johnson, A. S. (1990). Impact of phytoplankton-generated
788 surfactants on air-sea gas exchange. *Journal of Geophysical Research*, *J. Geophys. Res.-Oceans*, 95(C3),
789 3337–3352, 1990.
- 790 Frew, N. M., Bock, E. J., McGillis, W. R., Karachintsev, A. V., Hara, T., Münsterer, T., and Jähne, B.: Variation
791 of air-water gas transfer with wind stress and surface viscoelasticity, in: *Air-Water Gas Transfer*, 529–541,
792 1995.
- 793 Frew, N. M., Bock, E. J., Schimpf, U., Hara, T., Haußecker, H., Edson, J. B., ... and Jähne, B. (2004). Air-sea
794 gas transfer: Its dependence on wind stress, small-scale roughness, and surface films. *Journal of Geophysical*
795 *Research*, *J. Geophys. Res.-Oceans*, 109(C8), C08S17, <https://doi.org/10.1029/2003JC002131>, 2004.
- 796 Frka, S., Dautović, J., Kozarac, Z., Čosović, B., Hoffer, A., and Kiss, G. (2012). Surface-active substances in
797 atmospheric aerosol: an electrochemical approach. *Tellus B: Chemical and Physical Meteorology*, 64(1),
798 18490, <https://doi.org/10.3402/tellusb.v64i0.18490>, 2012.
- 799 Gade, M., Alpers, W., Hühnerfuss, H., & Lange, P. A. (1998). Wind wave tank measurements of wave
800 damping and radar cross sections in the presence of monomolecular surface films. *Journal of Geophysical*
801 *Research*, *J. Geophys. Res.-Oceans*, 103(C2), 3167–3178, 1998.
- 802 Gašparović, B., and Čosović, B. (2003). Surface-active properties of organic matter in the North Adriatic Sea.
803 *Estuarine, Coastal and Estuar. Coast. Shelf Science*, *Sci.*, 58(3), 555–566, 2003.
- 804 Hühnerfuss, H., Alpers, W., Lange, P. A., & Walter, W. (1981). Attenuation of wind waves by artificial
805 surface films of different chemical structure. *Geophysical Research Letters*, *Geophys. Res. Lett.*, 8(11), 1184–
806 1186, 1981.
- 807 Hunter, K. A., and Liss, P. S. (1981). Organic sea surface films. In, in: *Elsevier oceanography series*
808 *(Oceanography Series*, Vol. 31, pp-259–298), Elsevier, 1981.
- 809 Jähne, B., Münnich, K. O., Bössinger, R., Dutzi, A., Huber, W., and Libner, P. (1987). On the parameters
810 influencing air-water gas exchange. *Journal of Geophysical Research*, *J. Geophys. Res.-Oceans*, 92(C2),
811 1937–1949, 1987.

- 812 Jenkinson, I. R., Seuront, L., Ding, H., and Elias, F.-(2018)-.: Biological modification of mechanical properties
813 of the sea surface microlayer, influencing waves, ripples, foam and air-sea fluxes-. *Elementa-Science of the*
814 *Anthropocene*, 6, 26, <https://doi.org/10.1525/elementa.262>, 2018.
- 815 Kiefhaber, D., Reith, S., Rocholz, R., and Jähne, B.-(2014)-.: High-speed imaging of short wind waves by shape
816 from refraction-. *Journal of the European Optical Society- J. Eur. Opt. Soc.-Rapid publications, Publ.*, 9, 14015,
817 <https://doi.org/10.2971/jeos.2014.14015>, 2014.
- 818 Kock, A., Schafstall, J., Dengler, M., Brandt, P., and Bange, H. W.-(2012)-.: Sea-to-air and diapycnal nitrous
819 oxide fluxes in the eastern tropical North Atlantic Ocean-. *Biogeosciences*, 9(3)-, 957-964,
820 <https://doi.org/10.5194/bg-9-957-2012>, 2012.
- 821 Krall, K. E.-(2013)-.: Laboratory ~~Investigations of Air-Sea Gas Transfer~~investigations of air-sea gas transfer
822 under a ~~Wide Range of Water Surface Conditions~~.wide range of water surface conditions, PhD
823 ~~thesis~~. Universität Heidelberg. DOI: 10.11588/heidok.00014392, Germany,
824 <https://doi.org/10.11588/heidok.00014392>, 2013.
- 825 Kunz, J.-(2027)-.: Active ~~Thermography~~thermography as a ~~Tool~~tool for the ~~Estimation of Air-Water Transfer~~
826 ~~Velocities~~.-Dissertation-estimation of air-water transfer velocities, PhD thesis, Universität Heidelberg.-DOI:
827 10.11588/heidok.00022903-, Germany, <https://doi.org/10.11588/heidok.00022903>, 2017.
- 828 Kurata, N., Vella, K., Hamilton, B., Shivji, M., Soloviev, A., Matt, S., ---and Perrie, W.-(2016)-.: Surfactant-
829 associated bacteria in the near-surface layer of the ocean-. *Scientific reports-, Sci. Rep.*, 6(4)-, 19123,
830 <https://doi.org/10.1038/srep19123>, 2016.
- 831 Kuznetsova, M.-, and Lee, C.-(2001)-.: Enhanced extracellular enzymatic peptide hydrolysis in the sea-surface
832 microlayer-. *Marine Chemistry-, Mar. Chem.*, 73(3-4)-, 319-332, 2001.
- 833 Kuznetsova, M., Lee, C., Aller, J., and Frew, N.-(2004)-.: Enrichment of amino acids in the sea surface
834 microlayer at coastal and open ocean sites in the North Atlantic Ocean-. *Limnology and Oceanography-, Limnol.*
835 *Oceanogr.*, 49(5)-, 1605-1619, 2004.
- 836 Laß, K.-, and Friedrichs, G.-(2011)-.: Revealing structural properties of the marine nanolayer from vibrational
837 sum frequency generation spectra-. *Journal of Geophysical Research: Oceans, 116(C8)-, J. Geophys. Res.-*
838 *Oceans*, 116, C08011, <https://doi.org/10.1029/2010JC006609>, 2011.
- 839 Laß, K., Bange, H. W., and Friedrichs, G.-(2013)-.: Seasonal signatures in SFG vibrational spectra of the sea
840 surface nanolayer at Boknis Eck Time Series Station (SW Baltic Sea)-. *Biogeosciences*, 10(8)-, 5325-5334-
841 <https://doi.org/10.5194/bg-10-5325-2013>, 2013.
- 842 Laxague, N. J. M., Zappa, C. J., Soumya, S., and Wurl, O.-(2024)-.: The suppression of ocean waves by biogenic
843 slicks-. *J. R. Soc. Interface*, 21-, 20240385, <https://doi.org/10.1098/rsif.2024.0385>, 2024.
- 844 Lindroth, P.-, and Mopper, K.-(1979)-.: High-performance liquid chromatographic determination of subpicomole
845 amounts of amino acids by precolumn fluorescence derivatization with o-phthalaldehyde-. *Analytical*
846 *Chemistry-, Anal. Chem.*, 51(11)-, 1667-1674, 1979.
- 847 Liu, K.-, and Dickhut, R. M.-(1998)-.: Effects of wind speed and particulate matter source on surface microlayer
848 characteristics and enrichment of organic matter in southern Chesapeake Bay-. *Journal of Geophysical Research:*
849 *Atmospheres-, J. Geophys. Res.-Atmos.*, 103(D9)-, 10571-10577, 1998.
- 850 Maßmig, M., Cisternas-Novoa, C., and Engel, A.-(2024)-.: Uncovering the role of oxygen on organic carbon
851 cycling: insights from a continuous culture study with a facultative anaerobic bacterioplankton species
852 (*Shewanella baltica*)-. *Frontiers in Marine Science-*, *Front. Mar. Sci.*, 11, 1328392,
853 <https://doi.org/10.3389/fmars.2024.1328392>, 2024.

- 854 McKenna, S. P., and Bock, E. J. (2006).: Physicochemical effects of the marine microlayer on air–sea gas
855 transport. In, in: *Marine Surface Films: Chemical Characteristics, Influence on Air–Sea Interactions and Remote*
856 *Sensing* (pp., 77–91). Springer, Berlin, Heidelberg: Springer Berlin Heidelberg, 2006.
- 857 Mesarchaki, E., Kräuter, C., Krall, K. E., Bopp, M., Helleis, F., Williams, J., and Jähne, B. (2015).: Measuring
858 air–sea gas-exchange velocities in a large-scale annular wind-wave tank. *Ocean Science, Sci.*, 11(1), 121–138,
859 <https://doi.org/10.5194/os-11-121-2015>, 2015.
- 860 Nagel, L., Krall, K. E., and Jähne, B. (2019).: Measurements of air–sea gas transfer velocities in the Baltic Sea.
861 *Ocean Science, Sci.*, 15(2), 235–247, <https://doi.org/10.5194/os-15-235-2019>, 2019.
- 862 Parsons, T. R., Stephens, K., and Strickland, J. D. H. (1964).: On the chemical composition of eleven species of
863 marine phytoplankters. *Journal of the Fisheries, J. Fish. Res. Board of Canada, Can.*, 18(6), 1001–1016, 1961.
- 864 Pereira, R., Ashton, I., Sabbaghzadeh, B., Shutler, J. D., and Upstill-Goddard, R. C. (2018).: Reduced air–sea
865 CO_2 exchange in the Atlantic Ocean due to biological surfactants. *Nature Geoscience, 11(7)*, *Nat. Geosci.*,
866 11, 492–496, <https://doi.org/10.1038/s41561-018-0136-2>, 2018.
- 867 Pogorzelski, S. J., Kogut, A. D., and Mazurek, A. Z. (2006).: Surface rheology parameters of source-specific
868 surfactant films as indicators of organic matter dynamics. *Hydrobiologia*, 554, 67–81, *Hydrobiologia*, 554, 67–
869 81, 2006. Reinthaler, T., Sintes, E., and Herndl, G. J. (2008). Dissolved organic matter and bacterial production
870 and respiration in the sea surface microlayer of the open Atlantic and the western Mediterranean Sea. *Limnology*
871 *and Oceanography*, 53(1), 122–136.
- 872 [Reinthaler, T., Sintes, E., and Herndl, G. J.: Dissolved organic matter and bacterial production and respiration in
873 the sea-surface microlayer of the open Atlantic and the western Mediterranean Sea, *Limnol. Oceanogr.*, 53, 122–
874 136, 2008.](https://doi.org/10.1002/lno.2008)
- 875 Ribas-Ribas, M., Helleis, F., Rahlff, J., & Wurl, O. (2018).: Air–sea CO_2 exchange in a large annular
876 wind-wave tank and the effects of surfactants. *Frontiers in Marine Science*, *Front. Mar. Sci.*, 5, 457,
877 <https://doi.org/10.3389/fmars.2018.00457>, 2018.
- 878 Sabbaghzadeh, B., Upstill-Goddard, R. C., Beale, R., Pereira, R., and Nightingale, P. D. (2017).: The Atlantic
879 Ocean surface microlayer from 50° N to 50° S is ubiquitously enriched in surfactants at wind speeds up to 13
880 m s⁻¹. *Geophysical Research Letters*, *Geophys. Res. Lett.*, 44(6), 2852–2858,
881 <https://doi.org/10.1002/2017GL072988>, 2017.
- 882 Santschi, P. H., Xu, C., Schwehr, K. A., Lin, P., Sun, L., Chin, W. C., and Quigg, A. (2020).: Can the
883 protein/carbohydrate (P/C) ratio of exopolymeric substances (EPS) be used as a proxy for their
884 “stickiness” and aggregation propensity? *Marine Chemistry*, *Mar. Chem.*, 218, 103734,
885 <https://doi.org/10.1016/j.marchem.2019.103734>, 2020.
- 886 Satpute, S. K., Banat, I. M., Dhakephalkar, P. K., Banpurkar, A. G., and Chopade, B. A. (2010).: Biosurfactants,
887 bioemulsifiers and exopolysaccharides from marine microorganisms. *Biotechnology Advances*, *Biotechnol.*
888 *Adv.*, 28(4), 436–450, 2010.
- 889 Schmidt, R., and Schneider, B. (2011).: The effect of surface films on the air–sea gas exchange in the Baltic
890 Sea. *Marine Chemistry*, *Mar. Chem.*, 126(1–4), 56–62, 2011.
- 891 [Schmundt, D., Münsterer, T., Lauer, H., and Jähne, B.: The circular wind-wave facilities at the University of
892 Heidelberg, in: Jähne, B. and Monahan, E. C. \(Eds.\), *Air–Water Gas Transfer*, AEON, Hanau, 505–516, 1995.](https://doi.org/10.1016/B978-3-90-000000-0.50000-0)
- 893 Shaharom, S., Latif, M. T., Khan, M. F., Yusof, S. N. M., Sulong, N. A., Wahid, N. B. A., and Suratman, S.
894 (2018).: Surfactants in the sea surface microlayer, subsurface water and fine marine aerosols in different
895 background coastal areas. *Environmental Science and Pollution Research*, *Environ. Sci. Pollut. Res.*, 25, 27074–
896 27089, 2018.

- 897 Sieburth, J. M.-(1983)-.: Microbiological and organic-chemical processes in the surface and mixed layers-, in:
898 Air-sea exchange-Sea Exchange of gasesGases and particlesParticles, 121-172, 1983.
- 899 Singh, A.-, and Tyagi, V. K.-(2014)-.: Arginine-based novel cationic surfactants: a review-, Tenside Surfactants
900 Detergents,Surf. Det., 51(3)-, 202-214-, 2014.
- 901 van Pinxteren, M., MüllerMüller, C., Iinuma, Y., Stolle, C., and Herrmann, H.-(2012)-.: Chemical
902 characterization of dissolved organic compounds from coastal sea surface microlayers (Baltic Sea, Germany)-
903 Environmental Science and Technology-, Environ. Sci. Technol., 46(19)-, 10455-10462, 2012.
- 904 Tang, S.-, and Wu, J. (1992). Suppression of wind-generated ripples by natural films: A laboratory study. Journal
905 of Geophysical Research: Oceans, 97(C4), 5301-5306.
- 906 Stefan, R. L. and Szeri, A. J.: Surfactant scavenging and surface deposition by rising bubbles, J. Colloid
907 Interface Sci., 212, 1-13, 1999.
- 908 Sun, C. C., Sperling, M., and Engel, A.-(2018)-.: Effect of wind speed on the size distribution of gel particles in
909 the sea surface microlayer: insights from a wind-wave channel experiment-, Biogeosciences, 15(11)-, 3577-
910 3589, <https://doi.org/10.5194/bg-15-3577-2018>, 2018.
- 911 Tang, S. and Wu, J.: Suppression of wind-generated ripples by natural films: a laboratory study, J. Geophys.
912 Res.-Oceans, 97, 5301-5306, 1992.
- 913 Tsai, W. T.-, and Liu, K. K.-(2003)-.: An assessment of the effect of sea surface surfactant on global atmosphere-
914 -ocean CO₂CO₂ flux-, Journal of Geophysical Research-, J. Geophys. Res.-Oceans, 108(C4)-25-, 3127,
915 <https://doi.org/10.1029/2000JC000740>, 2003.
- 916 Thornton, D. C.-(2014)-.: Dissolved organic matter (DOM) release by phytoplankton in the contemporary and
917 future ocean-, European Journal of Phycology-, Eur. J. Phycol., 49(1)-, 20-46, 2014.
- 918 Wanninkhof, R., Asher, W. E., Ho, D. T., Sweeney, C., and McGillis, W. R.-(2009)-.: Advances in quantifying
919 air-sea gas exchange and environmental forcing-, Annual Review of Marine Science-, 1(1)-, Annu. Rev. Mar.
920 Sci., 1, 213-244-, 2009.
- 921 Wurl, O.-, and Holmes, M.-(2008)-.: The gelatinous nature of the sea-surface microlayer-, Marine Chemistry-,
922 Mar. Chem., 110(1-2)-, 89-97, 2008.
- 923 Wei, Y.-, & and Wu, J.-(1992)-.: In situ measurements of surface tension, wave damping, and wind properties
924 modified by natural films-, Journal of Geophysical Research-, J. Geophys. Res.-Oceans, 97(C4)-, 5307-5313,
925 1992.
- 926 Wurl, O., Wurl, E., Miller, L., Johnson, K., and Vagle, S.-(2011)-.: Formation and global distribution of sea-
927 surface microlayers-, Biogeosciences, 8(1)-, 121-135, <https://doi.org/10.5194/bg-8-121-2011>, 2011.
- 928 Wurl, O., Stolle, C., Van Thuoc, C., Thu, P. T., and Mari, X.-(2016)-.: Biofilm-like properties of the sea surface
929 and predicted effects on air-sea CO₂CO₂ exchange-, Progress in Oceanography-, Prog. Oceanogr., 144, 15-24,
930 2016.
- 931 Xu, C., Zhang, S., Chuang, C. Y., Miller, E. J., Schwehr, K. A., and Santschi, P. H.-(2011)-.: Chemical
932 composition and relative hydrophobicity of microbial exopolymeric substances (EPS)-isolated by anion
933 exchange chromatography and their actinide-binding affinities-, Marine Chemistry-, Mar. Chem., 126(1-4)-, 27-
934 36, 2011.
- 935 Zäncker, B., Bracher, A., Röttgers, R., and Engel, A.-(2017)-.: Variations of the organic matter composition in
936 the sea surface microlayer: a comparison between open ocean, coastal, and upwelling sites off the Peruvian

937 coast. ~~Frontiers in Microbiology, 8, 2369, Front. Microbiol., 8, 2369, <https://doi.org/10.3389/fmicb.2017.02369>,~~
938 ~~2017.~~

939 Zhen, C., Ge, X. F., Lu, Y. T., and Liu, W. Z. ~~(2023).~~ ~~Chemical structure, properties and potential applications~~
940 ~~of surfactin, as well as advanced strategies for improving its microbial production.~~ AIMS
941 ~~Microbiology, Microbiol., 9(2), 195–214, 2023.~~

942 ~~Žutić~~Žutić, V., Ćosović, B., Marčenko, E., Bihari, N., and Kršinić, F. ~~(1981).~~ ~~Surfactant production by marine~~
943 ~~phytoplankton.~~ ~~Marine Chemistry, Mar. Chem., 10(6), 505–520, 1981.~~

944 65

945

946